



Spatial Generalized Linear Models in R Using **spmodel**

Michael Dumelle  Jay M. Ver Hoef  Matt Higham 
United States Alaska Fisheries
Environmental Protection Agency Science Center St. Lawrence University

Abstract

Non-Gaussian data are common in practice and include binary, count, skewed, and proportion data types. Often, non-Gaussian data are modeled using a generalized linear model (GLM). GLMs typically assume that observations are independent of one another. This is an impractical assumption for spatial data, as nearby observations tend to be more similar than distant ones. The **spmodel** package in R provides a suite of tools for fitting spatial generalized linear models (SPGLMs) to non-Gaussian data and making spatial predictions (i.e., Kriging). SPGLMs for point-referenced (x- and y-coordinates) support are fit using the `spglm()` function, while SPGLMs for areal (lattice, polygon) support are fit using the `spgautor()` function. Both `spglm()` and `spgautor()` maximize a novel Laplace likelihood which marginalizes over the model's fixed effects and latent mean while formally incorporating spatial covariance among observations. The inputs and outputs of `spglm()` and `spgautor()` closely resemble the `glm()` function from base R, easing the transition from GLMs to SPGLMs. **spmodel** provides and builds upon several commonly used helper functions for model building like `summary()`, `plot()`, and `fitted()`, among others. Spatial predictions of the latent mean at unobserved locations are obtained using `predict()` or `augment()`. **spmodel** accommodates myriad advanced modeling features like geometric anisotropy, nonspatial random effects, analysis of variance, and more. Throughout, we use **spmodel** to fit SPGLMs to moose presence and counts in Alaska, United States (US), skewed conductivity data in the Southwestern US, harbor seal abundance trends in Alaska, US, and voter turnout rates in Texas, US.

Keywords: autoregressive model, geostatistical model, Poisson regression, link function, logistic regression, overdispersion, spatial covariance, spatial dependence.

1. Introduction

In practice, non-Gaussian data (e.g., binary, count, skewed, and proportion data) are ubiquitous. Non-Gaussian data that belong to an exponential family can be naturally modeled using a generalized linear model (GLM) regression framework (Nelder and Wedderburn 1972; McCullagh and Nelder 1989). In a GLM, an $n \times 1$ response variable \mathbf{y} belongs to a statistical distribution (e.g., binomial, Poisson) with some mean and variance. Often, the analysis goal is to study the impact of a linear function of several explanatory variables on the mean of \mathbf{y} through a GLM. In this context, the latent (i.e., unobserved) mean of \mathbf{y} , $\boldsymbol{\mu}$, is linked to these explanatory variables via a link function:

$$f(\boldsymbol{\mu}|\mathbf{X}, \boldsymbol{\beta}) \equiv \mathbf{w} = \mathbf{X}\boldsymbol{\beta}, \quad (1)$$

where for a sample size n , $f(\cdot)$ is a link function that connects $\boldsymbol{\mu}$ to \mathbf{w} , \mathbf{X} is the $n \times p$ design matrix of explanatory variables, and $\boldsymbol{\beta}$ is the $p \times 1$ vector of fixed effects. While the mean is typically constrained in some way (e.g., if a probability, between zero and one), the link function generally makes \mathbf{w} unconstrained. Common link functions include the log odds (i.e., logit) link for binary and proportion data and the log link for count and skewed data. Equation 1 can also be written in terms of the inverse link function, $f^{-1}(\cdot)$:

$$\boldsymbol{\mu}|\mathbf{X}, \boldsymbol{\beta} \equiv f^{-1}(\mathbf{w}) = f^{-1}(\mathbf{X}\boldsymbol{\beta}).$$

The GLM fixed effects ($\boldsymbol{\beta}$) are typically estimated via maximum likelihood (Chambers and Hastie 1992). It is often convenient to compute the maximum likelihood estimates using the iteratively reweighted least squares (IRWLS) algorithm (Wood 2017), which is an approach used by the `glm()` function in the R programming language (R Core Team 2024). GLMs add an additional layer of complexity compared to linear regression models, as the left-hand side of Equation 1 is a function of the mean of \mathbf{y} rather than \mathbf{y} itself (as in linear regression models).

The standard GLM assumes the elements of \mathbf{y} are independent. This independence assumption is typically impractical for spatial data. For spatial data, nearby observations tend to be more similar than distant observations (Tobler 1970), which leads to positive spatial covariance among observations. The consequences of ignoring spatial covariance in statistical models for spatial data can be severe and include imprecise parameter estimates as well as misleading standard errors that inflate Type-I error rates and decrease power (Zimmerman and Ver Hoef 2024).

An approach for handling spatial data using a GLM is to assume the elements of \mathbf{w} exhibit both spatial and nonspatial variability. This is achieved by adding to Equation 1 two random effects, $\boldsymbol{\tau}$ and $\boldsymbol{\epsilon}$. The random effect $\boldsymbol{\tau}$ is an $n \times 1$ column vector of spatially dependent random errors. We assume that $E(\boldsymbol{\tau}) = \mathbf{0}$ and $Cov(\boldsymbol{\tau}) = \sigma_{\tau}^2 \mathbf{R}$, where $E(\cdot)$ and $Cov(\cdot)$ denote expectation and covariance, respectively. The variance parameter σ_{τ}^2 controls the magnitude of spatial covariance and is often called a partial sill. The matrix \mathbf{R} is an $n \times n$ spatial correlation matrix that depends on a range parameter controlling the distance-decay rate of the spatial correlation. One example of a spatial covariance matrix is the “exponential,” which is given by

$$Cov(\boldsymbol{\tau}) = \sigma_{\tau}^2 \mathbf{R}_{exp} = \sigma_{\tau}^2 \exp(-\mathbf{H}/\phi), \quad (2)$$

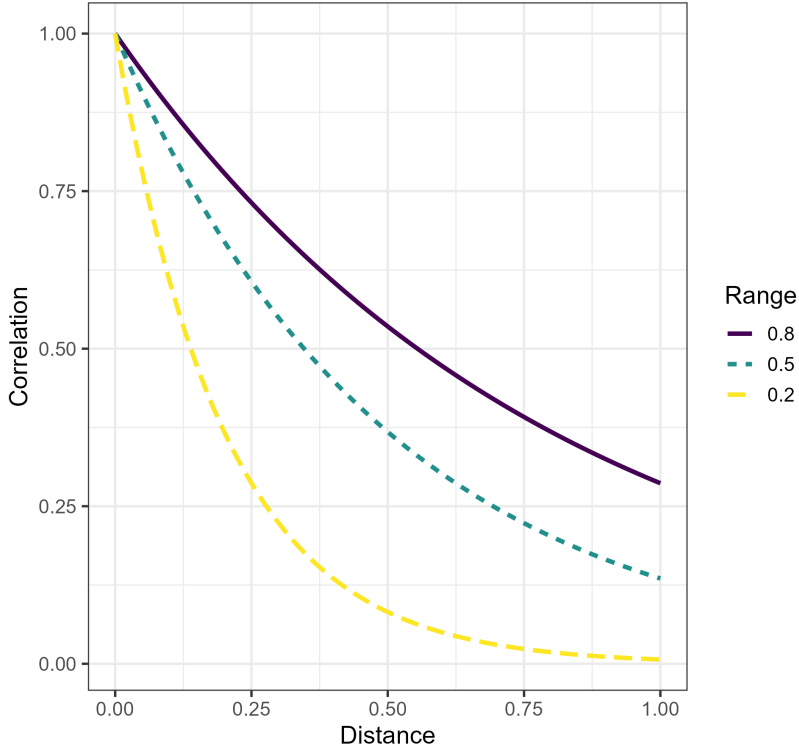


Figure 1: An exponential spatial correlation function with varying range parameters.

where \mathbf{H} is a matrix of pairwise distances among the elements of \mathbf{y} and ϕ is the range parameter. From Equation 2, as the distance between two elements of \mathbf{y} increases, the spatial covariance decreases, which reflects intuition. Moreover, as the range parameter, ϕ , increases, the strength of spatial dependence increases (Figure 1). The random effect $\boldsymbol{\epsilon}$ is an $n \times 1$ column vector of independent random errors. We assume that $E(\boldsymbol{\epsilon}) = \mathbf{0}$ and $Cov(\boldsymbol{\tau}) = \sigma_{\epsilon}^2 \mathbf{I}$, where \mathbf{I} is an $n \times n$ identity matrix. The variance parameter σ_{ϵ}^2 controls the magnitude of nonspatial variability (i.e., fine-scale variation) and is often called a nugget. Often in spatial statistics, quantities are explicitly referenced with respect to \mathbf{s} , a vector of spatial coordinates indexing the observation (Cressie 1993). For example, \mathbf{y} and \mathbf{X} may instead be written $\mathbf{y}(\mathbf{s})$ and $\mathbf{X}(\mathbf{s})$, respectively. We acknowledge the utility of this nomenclature but drop the explicit dependence on \mathbf{s} for simplicity of notation moving forward.

Through inclusion of $\boldsymbol{\tau}$ and $\boldsymbol{\epsilon}$, the spatial GLM (SPGLM) can be written as

$$f(\boldsymbol{\mu} | \mathbf{X}, \boldsymbol{\beta}, \boldsymbol{\tau}, \boldsymbol{\epsilon}) \equiv \mathbf{w} = \mathbf{X}\boldsymbol{\beta} + \boldsymbol{\tau} + \boldsymbol{\epsilon}. \quad (3)$$

Assuming independence among $\boldsymbol{\tau}$ and $\boldsymbol{\epsilon}$, it follows that

$$Cov(\boldsymbol{\tau} + \boldsymbol{\epsilon}) = Cov(\boldsymbol{\tau}) + Cov(\boldsymbol{\epsilon}) = \sigma_{\tau}^2 \mathbf{R} + \sigma_{\epsilon}^2 \mathbf{I}.$$

Henceforth, we refer to σ_{τ}^2 as σ_{de}^2 (for spatially dependent error variance) and σ_{ϵ}^2 as σ_{ie}^2 (for independent error variance). The parameters σ_{de}^2 , σ_{ie}^2 , and ϕ , in addition to any other parameters in \mathbf{R} , compose $\boldsymbol{\theta}$, the covariance parameter vector.

Fitting and using SPGLMs is challenging both conceptually and computationally (Bolker, Brooks, Clark, Geange, Poulsen, Stevens, and White 2009). Recently, however, there have

been numerous, significant advances in R software that have made these models more accessible to practitioners. The **brms** (Bürkner 2017), **carBayes** (Lee 2013), **ngspatial** (Hughes and Cui 2020), **R-INLA** (Lindgren and Rue 2015), **inlabru** (Bachl, Lindgren, Borchers, and Illian 2019), **spBayes** (Finley, Banerjee, and Carlin 2007), **spOccupancy** (Doser, Finley, Kéry, and Zipkin 2022), **spAbundance** (Doser, Finley, Kéry, and Zipkin 2024), and **spNNGP** (Finley, Datta, and Banerjee 2022) packages take a Bayesian approach, either directly sampling from posterior distributions of parameters (e.g., using MCMC) or approximating them. A benefit of Bayesian approaches is that prior information can be incorporated and uncertainty quantification of parameter estimates is straightforward. However, Bayesian approaches, especially those using MCMC, can be computationally expensive. In order to reduce computation time, many of these packages (e.g., **R-INLA**) work with the precision matrix instead of the covariance matrix so that computationally expensive matrix inversion is not required. Working with precision matrices, however, can be more restrictive and less intuitive than working with covariance matrices. The **FRK** (Sainsbury-Dale, Zammit-Mangion, and Cressie 2024), **glmmTMB** (Brooks, Kristensen, van Benthem, Magnusson, Berg, Nielsen, Skaug, Maechler, and Bolker 2017), **hglm** (Ronnegard, Shen, and Alam 2010), **mgev** (Wood 2017), and **spAMM** (Rousset and Ferdy 2014) packages directly use Laplace, quasi-likelihood, or reduced-rank approaches to estimate parameters. These direct approaches tend to be computationally efficient, as they don't rely on MCMC sampling. In contrast to the Bayesian approach, a drawback of these direct approaches is that prior information cannot be formally incorporated and covariance parameter uncertainty is more challenging to quantify. The **sdmTMB** (Anderson, Ward, English, Barnett, and Thorson 2024) package combines elements of **R-INLA**, **glmmTMB**, and Gaussian Markov random fields to fit a wide variety of SPGLMs, while **tinyVAST** (Thorson, Anderson, Goddard, and Rooper 2025) extends some of these models to multivariate or (dynamic) structural equation models.

Building from Evangelou, Zhu, and Smith (2011) and Bonat and Ribeiro Jr (2016), Ver Hoef, Blagg, Dumelle, Dixon, Zimmerman, and Conn (2024) proposed a novel approach for fitting SPGLMs that leverages the Laplace approximation while marginalizing over both the latent \mathbf{w} and the fixed effects (β). This approach performed well in a variety of simulation settings, generally having appropriate confidence interval coverage for the fixed effects and prediction interval coverage for \mathbf{w} at new locations. It also performed similarly to the Bayesian SPGLM approach in **spBayes** and the automatic differentiation SPGLM approach in **glmmTMB** but was much faster. At small sample sizes, the approach outperformed the approximate Bayesian SPGLM approach in **R-INLA** and had similar computational times. For moderate sample sizes, it performed similarly to **R-INLA**, though **R-INLA** was faster. The novel Laplace approach is particularly attractive for two reasons. First, it is general enough that it can be applied to any covariance structure (not just spatial). Second, after estimating the covariance parameters, analytical solutions exist for the fixed effects (and their standard errors) as well as predictions of the latent \mathbf{w} at new locations (and their standard errors).

The **spmodel** R package (Dumelle, Higham, and Ver Hoef 2023) recently released a full set of modeling tools for SPGLMs fit using the novel Laplace approach described by Ver Hoef *et al.* (2024). These modeling tools are approachable and mirror the familiar **glm()** syntax from base-R, making the transition from GLMs to SPGLMs relatively seamless. The **spglm()** function fits SPGLMs for point-referenced support (e.g., x- and y-coordinates representing point locations in a field; these models are sometimes called “geostatistical” models), while the **spgautor()** function fits SPGLMs for areal support (e.g., polygon boundaries representing

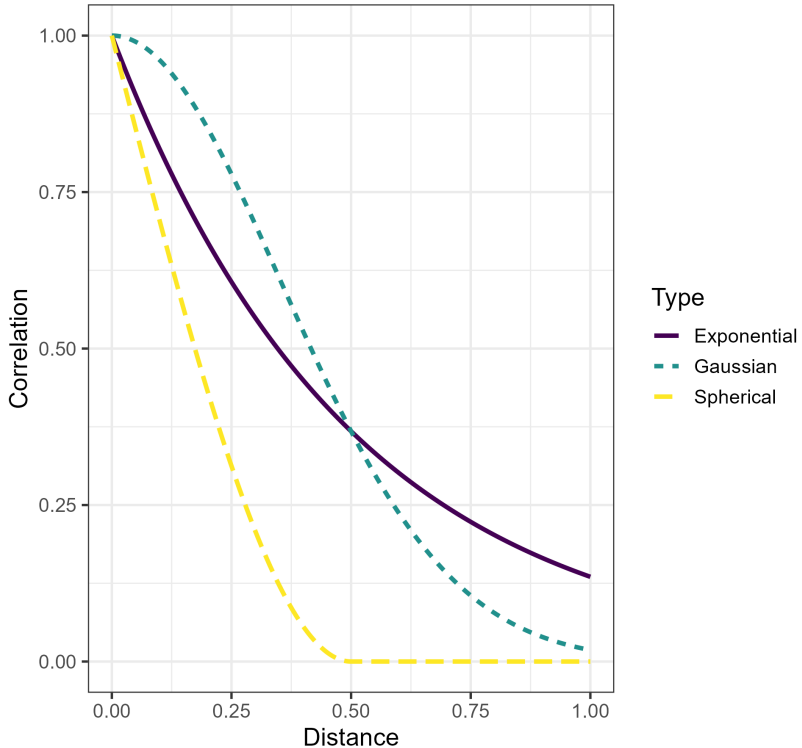


Figure 2: Exponential, Gaussian, and spherical spatial correlation functions all with range parameters equal to 0.5.

102 geographic subsets of a region; these models are sometimes called “autoregressive” models).
 103 For both point-referenced and areal supports, **spmodel** supports the binomial distribution for
 104 binary data, Poisson and negative binomial distributions for count data, Gamma and inverse
 105 Gaussian distributions for skewed data, and the beta distribution for proportion data. There
 106 are 20 different spatial covariance structures available including the exponential, Gaussian,
 107 and spherical for point-referenced support (Figure 2) and the conditional autoregressive, and
 108 simultaneous autoregressive structures for areal support **spmodel** provides tools for commonly
 109 used model summaries, visualizations, and diagnostics (e.g., fitted values) using standard R
 110 helper functions like `summary()`, `plot()`, and `fitted()`, among others. **spmodel** also pro-
 111 vides tools to predict `w` at new locations and quantify uncertainty in those prediction using
 112 `predict()` and `augment()`. This core functionality, combined with several advanced fea-
 113 tures we describe throughout the manuscript, enables **spmodel** to introduce novel, important
 114 SPGLM modeling tools previously missing from the existing R ecosystem.
 115 Of the existing R packages for SPGLMs, **spmodel** (version 0.11.1) is arguably most similar
 116 to **sdmTMB** (version 0.7.4) in terms of scope and feel. Both packages use similar syntax
 117 as `glm()`, accommodate flexible `formula` arguments (e.g., offsets, splines), handle spatial
 118 covariance that decays at different rates in different directions (i.e., geometric anisotropy),
 119 incorporate nonspatial random effects, support other R packages for modeling like **broom**
 120 (Robinson, Hayes, and Couch 2021; Kuhn and Silge 2022), **emmeans** (Lenth 2024), and **car**
 121 (Fox and Weisberg 2019), and have tools for model summaries, prediction, and simulating
 122 data. There are some notable differences between the two packages, however. **sdmTMB** sup-

123 ports several additional GLM distributions like the Tweedie, supports Hurdle models, and
124 can incorporate prior information through Bayesian applications. **sdmTMB** also provides
125 tools for working with temporal data and spatiotemporal data and provides enhanced vi-
126 sualizations of the model's marginal effects. **sdmTMB** does require a preprocessing step of
127 constructing a mesh prior to model fitting (using the stochastic partial differential equation
128 approach), and the density of the mesh can affect model results and computational com-
129 plexity. On the other hand, **spmodel** does not require the construction of a mesh prior to
130 model fitting. **spmodel** supports 20 different spatial covariances and models them directly,
131 rather than using a precision matrix approximation to the Matérn spatial covariance as in
132 **sdmTMB**. **spmodel** can model data directly using neighborhood distance and autoregressive
133 models, rather than relying on the polygon centroid (as in **sdmTMB**), which may not be
134 within the polygon's boundaries. **spmodel** provides experimental design tools (e.g., analysis
135 of variance, contrasts), supports **sf** objects in modeling and prediction functions ([Pebesma 2018](#)), has several specialized model diagnostics like leverage values and Cook's distances, and
136 has analytic solutions for fixed effect and prediction standard errors. Other similarities and
137 differences do exist between **sdmTMB** and **spmodel**, and both packages continue to evolve.
138 Overall, we believe that these packages are complementary and enhance the suite of SPGLM
139 tools accessible to practitioners.

141 The rest of this article is organized as follows. In Section 2, we provide some background for
142 the SPGLM fitting and prediction routines in **spmodel**. In Section 3, we provide an overview
143 of core SPGLM functionality in **spmodel** by modeling moose presence in Alaska, United
144 States (US). In Section 4, we model moose counts in Alaska, US; skewed lake conductivity
145 in the Southwestern US; harbor seal abundance trend behavior in Alaska, US; and voter
146 turnout rates in Texas, US. And in Section 5, we end with a discussion synthesizing **spmodel**'s
147 contributions to SPGLMs in R.

2. The spatial generalized linear model and marginalization

148 The novel Laplace approach implemented in **spmodel** formally maximizes a hierarchical GLM
149 likelihood ([Lee and Nelder 1996](#); [Wood 2017](#)), making likelihood-based statistics for model
150 comparison like AIC ([Akaike 1974](#)), AICc ([Hoeting, Davis, Merton, and Thompson 2006](#)), BIC
151 ([Schwarz 1978](#)), deviance ([McCullagh and Nelder 1989](#)), and likelihood ratio tests available.
152 These types of statistics are not available for quasi-likelihood ([Wedderburn 1974](#); [Breslow](#)
153 and [Clayton 1993](#)) or pseudo-likelihood approaches ([Wolfinger and O'Connell 1993](#)), which
154 only specify the first two moments of a distribution. Next, we describe a brief overview of
155 the approach and how it can be used for several primary data analysis tasks ([Tredennick,](#)
156 [Hooker, Ellner, and Adler 2021](#)) like model comparison, parameter estimation, inference,
157 model diagnostics, and prediction.

158 2.1. Formulating the hierarchical likelihood

159 We can write the SPGLM likelihood hierarchically as

$$[\mathbf{y}|\mathbf{X}, \varphi, \boldsymbol{\theta}] = \int_{\mathbf{w}} \int_{\boldsymbol{\beta}} [\mathbf{y}|f^{-1}(\mathbf{w}), \varphi] [\mathbf{w}|\mathbf{X}, \boldsymbol{\beta}, \boldsymbol{\theta}] d\boldsymbol{\beta} d\mathbf{w}, \quad (4)$$

160 where $[\mathbf{y}|f^{-1}(\mathbf{w}), \varphi]$ is the density for the appropriate response distribution of \mathbf{y} (e.g., bi-
161 nomial, Poisson) given the latent \mathbf{w} and dispersion parameter (φ), and $[\mathbf{w}|\mathbf{X}, \boldsymbol{\beta}, \boldsymbol{\theta}]$ is the

¹⁶² multivariate Gaussian density for \mathbf{w} given the explanatory variables (\mathbf{X}), fixed effects ($\boldsymbol{\beta}$),
¹⁶³ and spatial covariance parameters ($\boldsymbol{\theta}$). The elements of $[\mathbf{y}|f^{-1}(\mathbf{w}), \varphi]$ are conditionally in-
¹⁶⁴ dependent (given \mathbf{w}), but the elements of $[\mathbf{w}|\mathbf{X}, \boldsymbol{\beta}, \boldsymbol{\theta}]$ share spatial covariance. Following
¹⁶⁵ Harville (1974), we can integrate $\boldsymbol{\beta}$ out of Equation 4, which yields

$$[\mathbf{y}|\mathbf{X}, \varphi, \boldsymbol{\theta}] = \int_{\mathbf{w}} [\mathbf{y}|f^{-1}(\mathbf{w}), \varphi][\mathbf{w}|\mathbf{X}, \boldsymbol{\theta}]d\mathbf{w}, \quad (5)$$

¹⁶⁶ where $[\mathbf{w}|\mathbf{X}, \boldsymbol{\theta}]$ is the restricted (i.e., residual) multivariate Gaussian density (Patterson and
¹⁶⁷ Thompson 1971) for \mathbf{w} given the explanatory variables and covariance parameters. The
¹⁶⁸ restricted multivariate Gaussian density is given by

$$[\mathbf{w}|\mathbf{X}, \boldsymbol{\theta}] = \frac{\exp(-\frac{1}{2}(\mathbf{y} - \mathbf{X}\tilde{\boldsymbol{\beta}})\Sigma^{-1}(\mathbf{y} - \mathbf{X}\tilde{\boldsymbol{\beta}})^{\top})}{(2\pi)^{(n-p)/2}|\Sigma|^{1/2}|\mathbf{X}^{\top}\Sigma^{-1}\mathbf{X}|^{1/2}},$$

¹⁶⁹ where $\tilde{\boldsymbol{\beta}} = (\mathbf{X}^{\top}\Sigma^{-1}\mathbf{X})^{-1}\mathbf{X}^{\top}\Sigma^{-1}\mathbf{w}$, Σ denotes the covariance matrix (of \mathbf{w}), and $|\cdot|$ denotes
¹⁷⁰ the determinant. Equation 5 can synonymously be written after profiling the overall variance
¹⁷¹ out of Σ , which reduces the dimension of $\boldsymbol{\theta}$ by one for optimization (Wolfinger, Tobias, and
¹⁷² Sall 1994). Next, let

$$\ell_{\mathbf{w}} = \log([\mathbf{y}|f^{-1}(\mathbf{w}), \varphi][\mathbf{w}|\mathbf{X}, \boldsymbol{\theta}])$$

¹⁷³ and rewrite Equation 5 as

$$[\mathbf{y}|\mathbf{X}, \varphi, \boldsymbol{\theta}] = \int_{\mathbf{w}} \exp(\ell_{\mathbf{w}})d\mathbf{w}.$$

¹⁷⁴ A second-order Taylor series expansion of $\ell_{\mathbf{w}}$ around a point \mathbf{w}^* yields

$$[\mathbf{y}|\mathbf{X}, \varphi, \boldsymbol{\theta}] \approx \int_{\mathbf{w}} \exp(\ell_{\mathbf{w}^*} + \mathbf{g}^{\top}(\mathbf{w} - \mathbf{w}^*) + \frac{1}{2}(\mathbf{w} - \mathbf{w}^*)^{\top}\mathbf{G}(\mathbf{w} - \mathbf{w}^*))d\mathbf{w},$$

¹⁷⁵ where \mathbf{g} and \mathbf{G} are the gradient and Hessian, respectively, of $\ell_{\mathbf{w}}$ with respect to \mathbf{w} . If \mathbf{w}^* is
¹⁷⁶ a value for which $\mathbf{g} = \mathbf{0}$,

$$[\mathbf{y}|\mathbf{X}, \varphi, \boldsymbol{\theta}] \approx \exp(\ell_{\mathbf{w}^*}) \int_{\mathbf{w}} \exp(-\frac{1}{2}(\mathbf{w} - \mathbf{w}^*)^{\top}(-\mathbf{G})(\mathbf{w} - \mathbf{w}^*))d\mathbf{w}. \quad (6)$$

¹⁷⁷ The integral in Equation 6 can be solved by leveraging properties of the normalizing constant
¹⁷⁸ of a multivariate Gaussian distribution. Thus, rewriting $\exp(\ell_{\mathbf{w}^*})$ yields

$$[\mathbf{y}|\mathbf{X}, \varphi, \boldsymbol{\theta}] \approx [\mathbf{y}|f^{-1}(\mathbf{w}^*), \varphi][\mathbf{w}^*|\mathbf{X}, \boldsymbol{\theta}](2\pi)^{n/2}|-\mathbf{G}_{\mathbf{w}^*}|^{-1/2},$$

¹⁷⁹ which can be directly evaluated. This result suggests a doubly iterative optimization over 1)
¹⁸⁰ $\boldsymbol{\theta}$ and φ and 2) the latent \mathbf{w} (to find each set of \mathbf{w}^*), which ultimately yields the marginal
¹⁸¹ restricted maximum likelihood estimators $\hat{\varphi}$ and $\hat{\boldsymbol{\theta}}$ and their respective values of \mathbf{w}^* , which
¹⁸² we call $\hat{\mathbf{w}}$. Ver Hoef *et al.* (2024) provide further details, which includes explicit forms of \mathbf{g}
¹⁸³ and \mathbf{G} for various response distributions.

¹⁸⁴ 2.2. Estimating fixed effects

We can estimate the fixed effects using generalized least squares (GLS) principles, a common practice for linear models estimated using restricted maximum likelihood methods. Had we observed \mathbf{w} , a GLS estimator for β is given by

$$\hat{\beta} = (\mathbf{X}^\top \Sigma^{-1} \mathbf{X})^{-1} \mathbf{X}^\top \Sigma^{-1} \mathbf{w} = \mathbf{B}\mathbf{w},$$

where $\mathbf{B} = (\mathbf{X}^\top \Sigma^{-1} \mathbf{X})^{-1} \mathbf{X}^\top \Sigma^{-1}$. While we do not \mathbf{w} , we do estimate it via $\hat{\mathbf{w}}$, and thus it is reasonable to define $\hat{\beta} = \mathbf{B}\hat{\mathbf{w}}$. To derive properties of $\hat{\beta}$ like expectation and variance, we must derive these properties for $\hat{\mathbf{w}}$ by conditioning on \mathbf{w} as if it were observed and leveraging the laws of total expectation and variance. Based on asymptotic properties of (restricted) maximum likelihood estimators (Cressie and Lahiri 1993), we may assume that given \mathbf{w} , $\hat{\mathbf{w}}$ has mean \mathbf{w} and variance equal to $-\mathbf{H}^{-1}$, the negative inverse Hessian (i.e., the inverse observed information matrix). Thus it follows that $E(\hat{\mathbf{w}})$ is given by

$$E(\hat{\mathbf{w}}) = E(E(\hat{\mathbf{w}}|\mathbf{w})) = E(\mathbf{w}) = \mathbf{X}\beta$$

and $\text{Var}(\hat{\mathbf{w}})$ is given by

$$\begin{aligned} \text{Var}(\hat{\mathbf{w}}) &= E(\text{Var}(\hat{\mathbf{w}}|\mathbf{w})) + \text{Var}(E(\hat{\mathbf{w}}|\mathbf{w})) \\ &= E(-\mathbf{H}^{-1}) + \text{Var}(\mathbf{w}) \\ &= -\mathbf{H}^{-1} + \Sigma \end{aligned}$$

Putting this all together, it follows that $\hat{\beta}$ is unbiased for β :

$$E(\hat{\beta}) = E(\mathbf{B}\hat{\mathbf{w}}) = \mathbf{B}E(\hat{\mathbf{w}}) = (\mathbf{X}^\top \Sigma^{-1} \mathbf{X})^{-1} (\mathbf{X}^\top \Sigma^{-1} \mathbf{X})\beta = \beta.$$

Moreover, it follows that

$$\begin{aligned} \text{Var}(\hat{\beta}) &= \text{Var}(\mathbf{B}\hat{\mathbf{w}}) \\ &= \mathbf{B}\text{Var}(\hat{\mathbf{w}})\mathbf{B}^\top \\ &= \mathbf{B}(-\mathbf{H}^{-1} + \Sigma)\mathbf{B}^\top \\ &= \mathbf{B}(-\mathbf{H})^{-1}\mathbf{B}^\top + \mathbf{B}\Sigma\mathbf{B}^\top \\ &= \mathbf{B}(-\mathbf{H})^{-1}\mathbf{B}^\top + (\mathbf{X}^\top \Sigma^{-1} \mathbf{X})^{-1}. \end{aligned}$$

In practice, $\text{Var}(\hat{\beta})$ is estimated by evaluating Σ at $\hat{\theta}$, the estimated covariance parameter vector.

These results are important because they justify analytic (i.e., closed-form) solutions for $\hat{\beta}$ and its associated variance. Analytic solutions are useful because they bypass the need for sampling-based strategies to evaluate the mean and variance of $\hat{\beta}$, a common technique for other approaches to SPGLMs like Bayesian MCMC that can be computationally intensive.

2.3. Inspecting model diagnostics

Inspecting model diagnostics is an important step of the modeling process that can yield valuable insights into model behavior and unusual observations. Montgomery, Peck, and Vining (2021) contextualize three components of unusual observations: outliers, leverage, and influence. An observation is an outlier if it has an extreme response value relative to

209 expectation. The response GLM residuals simply compare the observation to its fitted latent
 210 mean:

$$\mathbf{r}_r = \mathbf{y} - f^{-1}(\hat{\mathbf{w}})$$

211 Because observations often have a unique support in a GLM (e.g., only two possible response
 212 values for binary data) and the variance of an observation generally depends on its mean,
 213 response residuals lack some utility. Deviance residuals are a function of response residuals
 214 that are appropriately scaled to behave more like response residuals in a standard linear
 215 model. Deviance residuals are given by

$$\mathbf{r}_d = sign(\mathbf{r}_r)\sqrt{\mathbf{d}},$$

216 where \mathbf{d} is a vector of individual deviances. The sum of the squared deviance residuals equals
 217 the sum of the elements of \mathbf{d} , known as the deviance of the model fit. The deviance of the
 218 model fit quantifies twice the difference in log likelihoods between the a saturated model that
 219 fits every observation perfectly (i.e., $y_i = f^{-1}(\hat{w}_i)$ for all i) and the fitted model (Myers,
 220 Montgomery, Vining, and Robinson 2012). Deviance is often used as a fit statistic; lower
 221 values of deviance imply a better model fit (compared to the observed data). Pearson and
 222 standardized residuals are other types of GLM residuals that involve a scaling of the response
 223 residuals. The Pearson residuals scale \mathbf{r}_r by the square root of \mathbf{V} , a diagonal matrix with
 224 i th diagonal element equal to the variance of the response distribution evaluated at $f^{-1}(\hat{w}_i)$
 225 (Faraway 2016); \mathbf{V} is sometimes called the GLM weight matrix. The standardized residuals
 226 scale the deviance residuals by $\frac{1}{\sqrt{(1-\mathbf{L}_{ii})}}$, where \mathbf{L}_{ii} is the i th diagonal element of the leverage
 227 matrix, which we discuss next.

228 An observation has high leverage if its combination of explanatory variables is far away from
 229 other observations. In a linear model, the leverage (i.e., hat) values are the diagonal of the
 230 leverage (i.e., projection, hat) matrix, $\mathbf{L} = \mathbf{X}(\mathbf{X}^\top \mathbf{X})^{-1}\mathbf{X}^\top$. In a GLM, the leverage matrix is
 231 given by

$$\mathbf{L} = \mathbf{V}^{1/2} \mathbf{X} (\mathbf{X}^\top \mathbf{V} \mathbf{X})^{-1} \mathbf{X}^\top \mathbf{V}^{1/2}.$$

232 The larger the value of \mathbf{L}_{ii} , the more severe the leverage from the i th observation.
 233 An observation is influential if it has a sizable impact on model fit. Influence is measured
 234 using Cook's distance (Cook 1979; Cook and Weisberg 1982), which is given for a GLM by

$$\mathbf{c} = \frac{\mathbf{r}_s^2}{\text{tr}(\mathbf{L})} \frac{\text{diag}(\mathbf{L})}{(1 - \text{diag}(\mathbf{L}))},$$

235 where \mathbf{r}_s^2 are the standardized residuals and $\text{diag}(\mathbf{L})$ indicates the diagonal elements of the
 236 leverage matrix. The larger the value of c_i , the more severe the influence from the i th obser-
 237 vation. Montgomery *et al.* (2021) provide guidance for interpreting these types of statistics,
 238 including cutoffs to consider when identifying extreme residual, leverage, or influence values.
 239 In a linear model, the R^2 (R-squared) statistic quantifies the proportion of variability in the
 240 data captured by the explanatory variables. It is calculated as one minus the ratio of the error
 241 sum of squares to the total sum of squares (Rencher and Schaalje 2008). In a GLM, there
 242 are many ways to define a statistic that emulates the aforementioned meaning of R^2 from the
 243 linear model (Smith and McKenna 2013). This statistic is called a pseudo R-squared (PR^2).

²⁴⁴ One PR^2 for GLMs simply replaces the sums of squares ratio from the linear model with the
²⁴⁵ deviance ratio:

$$PR^2 = 1 - \frac{\text{deviance}_{\text{error}}}{\text{deviance}_{\text{total}}},$$

²⁴⁶ where $\text{deviance}_{\text{error}}$ is the deviance of the fitted model (sometimes called the error or residual
²⁴⁷ deviance) and $\text{deviance}_{\text{total}}$ is the deviance of the intercept-only model (sometimes called the
²⁴⁸ total or null deviance). In practice, $\text{deviance}_{\text{total}}$ is derived by computing $\hat{\mathbf{w}}$ when $\mathbf{X} \equiv \mathbf{1}$
²⁴⁹ (a column of all ones), given $\hat{\boldsymbol{\theta}}$ and $\hat{\varphi}$ from the fitted model. Like R^2 , PR^2 can be adjusted
²⁵⁰ to account for the numbers of parameters estimated in a model. Because the $\text{deviance}_{\text{total}}$
²⁵¹ denominator changes across fitted models (as the values of $\hat{\boldsymbol{\theta}}$ and $\hat{\varphi}$ change), this statistic
²⁵² should not be used as a model comparison tool. Rather, it should be used as an informative
²⁵³ diagnostic tool that is unique to each model fit and describes how much variability from that
²⁵⁴ model is attributable to the explanatory variables.

²⁵⁵ 2.4. Predicting at new locations

²⁵⁶ We may also predict values of the latent mean (on the link scale) at new locations by leveraging
²⁵⁷ the spatial covariance between observed locations and new locations (spatial prediction is
²⁵⁸ also called Kriging; see [Cressie \(1990\)](#)). Like in Section 2.2, suppose first that we observed
²⁵⁹ \mathbf{w} and we want to make predictions at \mathbf{u} , a vector of latent means at the new locations that
²⁶⁰ follows the same SPGLM from Equation 3 and has design matrix, \mathbf{X}_u . The vector $(\mathbf{w}, \mathbf{u})^\top$
²⁶¹ has expectation $(\mathbf{X}\boldsymbol{\beta}, \mathbf{X}_u\boldsymbol{\beta})^\top$ and covariance matrix $\begin{bmatrix} \Sigma & \Sigma_{\mathbf{w}\mathbf{u}} \\ \Sigma_{\mathbf{u}\mathbf{w}} & \Sigma_{\mathbf{u}\mathbf{u}} \end{bmatrix}$, where $\Sigma = \text{Var}(\mathbf{w}, \mathbf{w})$,
²⁶² $\Sigma_{\mathbf{w}\mathbf{u}} = \text{Var}(\mathbf{w}, \mathbf{u})$, $\Sigma_{\mathbf{u}\mathbf{w}} = \Sigma_{\mathbf{w}\mathbf{u}}^\top$ and $\Sigma_{\mathbf{u},\mathbf{u}} = \text{Var}(\mathbf{u}, \mathbf{u})$. Thus we may derive the conditional
²⁶³ distribution of $\mathbf{u}|\mathbf{w}$, which has the following properties:

$$\begin{aligned} E(\mathbf{u}|\mathbf{w}) &= \mathbf{X}_u\boldsymbol{\beta} + \Sigma_{\mathbf{u},\mathbf{w}}\Sigma^{-1}(\mathbf{w} - \mathbf{X}\boldsymbol{\beta}) \\ \text{Var}(\mathbf{u}|\mathbf{w}) &= \Sigma_{\mathbf{u},\mathbf{u}} - \Sigma_{\mathbf{u},\mathbf{w}}\Sigma^{-1}\Sigma_{\mathbf{w},\mathbf{u}} \end{aligned}$$

²⁶⁴ Recall, however, that we do not actually observe \mathbf{w} and instead compute $\hat{\mathbf{w}}$; so, to predict
²⁶⁵ \mathbf{u} and quantify its uncertainty, we must again leverage the laws of total expectation and
²⁶⁶ variance. [Ver Hoef et al. \(2024\)](#) show that $\hat{\mathbf{u}}$ and its associated variance are given by:

$$\begin{aligned} \hat{\mathbf{u}} &= \mathbf{X}_u\hat{\boldsymbol{\beta}} + \Sigma_{\mathbf{u},\mathbf{w}}\Sigma^{-1}(\hat{\mathbf{w}} - \mathbf{X}\hat{\boldsymbol{\beta}}) \\ \text{Var}(\hat{\mathbf{u}}) &= \Sigma_{\mathbf{u},\mathbf{u}} - \Sigma_{\mathbf{u},\mathbf{w}}\Sigma^{-1}\Sigma_{\mathbf{w},\mathbf{u}} + \mathbf{K}(\mathbf{X}^\top\Sigma^{-1}\mathbf{X})^{-1}\mathbf{K}^\top + \boldsymbol{\Lambda}(-\mathbf{H})^{-1}\boldsymbol{\Lambda}^\top, \end{aligned}$$

²⁶⁷ where $\mathbf{K} = \mathbf{X}_u - \Sigma_{\mathbf{u},\mathbf{w}}\Sigma^{-1}\mathbf{X}$ and $\boldsymbol{\Lambda} = \mathbf{X}_u\mathbf{B} + \Sigma_{\mathbf{u},\mathbf{w}}\Sigma^{-1}(\mathbf{1} - \mathbf{X}\mathbf{B})$ for a vector of ones, $\mathbf{1}$. As
²⁶⁸ with $\hat{\boldsymbol{\beta}}$, these covariance matrices are evaluated at $\hat{\boldsymbol{\theta}}$ in practice.

3. Modeling moose presence in Alaska, USA

²⁶⁹ The `moose` data in **spmodel** contain information on moose (*Alces Alces*) presence in the Togiak
²⁷⁰ region of Alaska, USA. `moose` is an `sf` object, a special data frame that is supplemented with
²⁷¹ spatial information using the `sf` package in R ([Pebesma 2018](#)). After loading **spmodel**, the
²⁷² first few rows of `moose` look like:

```
R> library("spmodel")

R> head(moose)

Simple feature collection with 6 features and 4 fields
Geometry type: POINT
Dimension:     XY
Bounding box:  xmin: 281896.4 ymin: 1518398 xmax: 311325.3 ymax: 1541016
Projected CRS: NAD83 / Alaska Albers
# A tibble: 6 x 5
  elev strat count presence      geometry
  <dbl> <chr> <dbl> <fct>       <POINT [m]>
1 469. L     0 0   (293542.6 1541016)
2 362. L     0 0   (298313.1 1533972)
3 173. M     0 0   (281896.4 1532516)
4 280. L     0 0   (298651.3 1530264)
5 620. L     0 0   (311325.3 1527705)
6 164. M     0 0   (291421.5 1518398)
```

273 There are five columns in `moose`: `elev`, the numeric site elevation (meters); `strat` a stratification variable for sampling with two levels ("L" and "M") categorized by landscape metrics
 274 at each site; `count`, the number of moose at each site; `presence`, a factor that indicates
 275 whether at least one moose was observed at each site (0 implies no moose; 1 implies at least
 276 one moose); and `geometry`, the NAD83/Alaska Albers (EPSG: 3338) projected coordinate of
 277 each site. These data have point-referenced support because each observation occurs at point
 278 coordinates represented by a POINT geometry. Moose are most prevalent in the southwestern
 279 and eastern parts of the Togiak region (Figure 3).

281 The `moose_preds` data in `spmodel` is an `sf` object with point locations at which moose
 282 presence predictions are desired. Like `moose`, `moose_preds` contains `elev` and `strat` for each
 283 site:

```
R> head(moose_preds)

Simple feature collection with 6 features and 2 fields
Geometry type: POINT
Dimension:     XY
Bounding box:  xmin: 291839.8 ymin: 1436192 xmax: 401239.6 ymax: 1512103
Projected CRS: NAD83 / Alaska Albers
# A tibble: 6 x 3
  elev strat      geometry
  <dbl> <chr>    <POINT [m]>
1 143. L     (401239.6 1436192)
2 324. L     (352640.6 1490695)
3 158. L     (360954.9 1491590)
4 221. M     (291839.8 1466091)
5 209. M     (310991.9 1441630)
6 218. L     (304473.8 1512103)
```

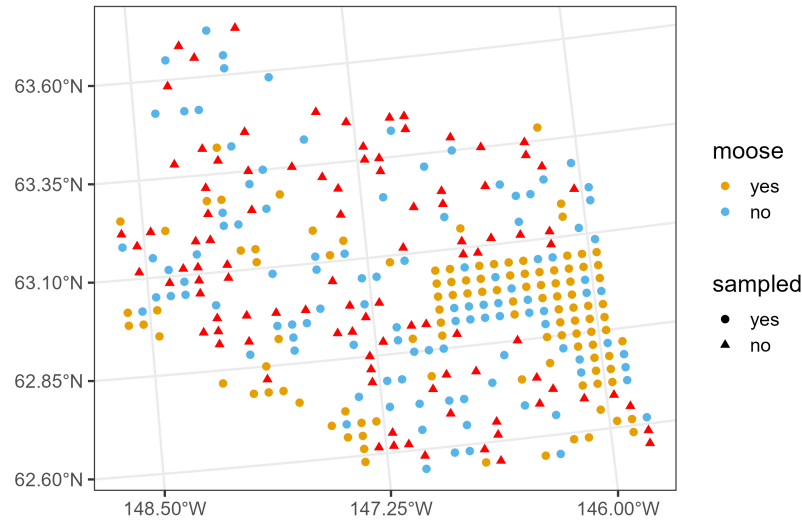


Figure 3: Moose presence in Alaska. Circles represent moose presence or absence (based on color) and triangles represent locations at which moose presence probability predictions are desired.

284 3.1. Model Fitting

285 SPGLMs in **spmodel** for point-referenced support are fit using the **spglm()** function. The
 286 **spglm()** function requires four arguments: **formula**, the relationship between the response
 287 and explanatory variables; **family**, the response distribution assumed for the response vari-
 288 able; **data**, the data frame that contains the variables in **formula**, and **spcov_type**, the type
 289 of spatial covariance. The **formula**, **family**, and **data** arguments are familiar because they
 290 are the three required arguments to **glm()** for nonspatial GLMs. So the transition from **glm()**
 291 to **spglm()** simply requires one additional argument: **spcov_type**. When **data** is not an **sf**
 292 object, **spglm()** also requires the **xcoord** and **ycoord** arguments, which indicate the columns
 293 in **data** that represent the projected x- and y-coordinates, respectively.

294 We use **spglm()** to fit a SPGLM (i.e., here, a spatial logistic regression model) quantifying
 295 the effect of elevation and strata on moose presence:

```
R> spbin <- spglm(
+   formula = presence ~ elev + strat,
+   family = binomial,
+   data = moose,
+   spcov_type = "exponential"
+ )
```

296 The **summary()** function returns a model summary with relevant information like the function
 297 call, deviance residuals, a coefficients table of fixed effects, the pseudo R-squared, spatial
 298 covariance parameters, and the GLM dispersion parameter (fixed at one in logistic regression):

```
R> summary(spbin)
```

```

Call:
spglm(formula = presence ~ elev + strat, family = binomial, data = moose,
      spcov_type = "exponential")

Deviance Residuals:
    Min      1Q  Median      3Q     Max 
-1.7535 -0.8005  0.3484  0.7893  1.5797 

Coefficients (fixed):
            Estimate Std. Error z value Pr(>|z|)    
(Intercept) -2.465713   1.486212 -1.659 0.097104 .  
elev         0.006036   0.003525  1.712 0.086861 .  
stratM       1.439273   0.420591  3.422 0.000622 *** 
---
Signif. codes:  0 '***' 0.001 '**' 0.01 '*' 0.05 '.' 0.1 ' ' 1

Pseudo R-squared: 0.06275

Coefficients (exponential spatial covariance):
        de      ie      range
5.145e+00 1.294e-03 4.199e+04

Coefficients (Dispersion for binomial family):
dispersion
      1

```

- 299 The model provides some evidence that elevation is positively associated with the log odds
 300 of moose presence (p value ≈ 0.087), after controlling for strata. The model also provides
 301 strong evidence that moose have a higher log odds of presence in the "M" strata compared to
 302 the "L" strata (p value < 0.001), after controlling for elevation.
 303 The fixed effects coefficients table from `summary()` is often of primary scientific interest, but
 304 it is not immediately usable when printed directly to the R console. The `tidy()` function
 305 tidies this table, turning it into a data frame (i.e., a tibble) with standard column names:

```

R> tidy(spbin, conf.int = TRUE)

# A tibble: 3 x 7
  term      estimate std.error statistic p.value conf.low conf.high
  <chr>      <dbl>     <dbl>     <dbl>    <dbl>    <dbl>     <dbl>
1 (Intercept) -2.47      1.49     -1.66  0.0971   -5.38e+0   0.447
2 elev        0.00604   0.00353     1.71  0.0869   -8.73e-4   0.0129
3 stratM      1.44       0.421     3.42  0.000622  6.15e-1    2.26

```

306 **3.2. Model Comparison**

307 The strength of spatial covariance in the data affects how beneficial an SPGLM is relative to
 308 a GLM. When the spatial covariance is strong, the SPGLM should notably outperform the
 309 GLM. When the spatial covariance is weak, the SPGLM and GLM should perform similarly.
 310 We can quantify the benefits of incorporating spatial covariance for a particular data set
 311 by comparing the fit of a SPGLM to a GLM. We can fit a GLM in **spmodel** by specifying
 312 `spcov_type = "none"`:

```
R> bin <- spglm(
+   formula = presence ~ elev + strat,
+   family = binomial,
+   data = moose,
+   spcov_type = "none"
+ )
R>
R> bin_glm <- glm(
+   formula = presence ~ elev + strat,
+   family = binomial,
+   data = moose,
+ )
R> round(coef(bin), digits = 4)

(Intercept)      elev      stratM
-0.4247     -0.0003     0.8070

R> round(coef(bin_glm), digits = 4)

(Intercept)      elev      stratM
-0.4247     -0.0003     0.8070

R> round(sqrt(diag(vcov(bin))), digits = 4)

(Intercept)      elev      stratM
 0.4208      0.0019     0.2906

R> round(sqrt(diag(vcov(bin_glm))), digits = 4)

(Intercept)      elev      stratM
 0.4208      0.0019     0.2906
```

313 Using `spglm()` instead of `glm()` ensures that **spmodel** helper functions are available and that
 314 each of the `spglm()` models uses the same hierarchical likelihood (Equation~4):

```
R> glance(spbin)

# A tibble: 1 x 10
  n      p  npqr value    AIC   AICc    BIC logLik deviance
  <int> <dbl> <int> <dbl> <dbl> <dbl> <dbl> <dbl> <dbl>
1  218     3     3  676.  682.  683.  693. -338.    176.
# i 1 more variable: pseudo.r.squared <dbl>
```

```
R> glance(bin)

# A tibble: 1 x 10
  n      p  npar value    AIC   AICc    BIC logLik deviance
  <int> <dbl> <int> <dbl> <dbl> <dbl> <dbl> <dbl>
1 218     3     0 708. 708. 708. -354.    294.
# i 1 more variable: pseudo.r.squared <dbl>
```

315 The likelihood-based statistics AIC, AICc, BIC, and deviance are much lower for the SPGLM,
 316 indicating a better fit relative to the GLM.

317 Instead of relying on likelihood-based statistics, models can be compared using a cross-
 318 validation procedure (James, Witten, Hastie, and Tibshirani 2013). The `loocv()` function
 319 performs leave-one-out cross validation, comparing the predicted mean (on the response scale)
 320 to the observed response variable for each hold-out observation, recomputing estimates of β
 321 in each iteration. Performing leave-one-out cross validation tends to be more computationally
 322 efficient than fitting the model, as leave-one-out cross validation requires only one set of prod-
 323 ucts involving the inverse covariance matrix (a primary computational burden), while fitting
 324 traditional models requires these products for each optimization iteration. After performing
 325 leave-one-out cross validation, statistics like bias, mean-squared-prediction error (MSPE), and
 326 the square root of MSPE (RMSPE) can be used to evaluate models:

```
R> loocv(spbin)

# A tibble: 1 x 3
  bias  MSPE RMSPE
  <dbl> <dbl> <dbl>
1 0.0000206 0.156 0.394
```

```
R> loocv(bin)

# A tibble: 1 x 3
  bias  MSPE RMSPE
  <dbl> <dbl> <dbl>
1 -1.23e-9 0.240 0.490
```

327 Both models have negligible bias, but the SPGLM has much lower MSPE and RMSPE than
 328 the GLM, indicating the SPGLM predictions are far more efficient. Both the likelihood-based
 329 leave-one-out cross validation metrics prefer the SPGLM to the GLM.

330 We may also want to compare the fit of two SPGLMs with different spatial covariance struc-
 331 tures. For example, we may want to compare the fit of an SPGLM with the "exponential"
 332 spatial covariance to the fit of a SPGLM with the "gaussian" spatial covariance:

```
R> spbin2 <- update(spbin, spcov_type = "gaussian")
R> glances(spbin, spbin2)
```

```
# A tibble: 2 x 11
  model      n     p   npar value    AIC   AICc    BIC logLik deviance
  <chr> <int> <dbl> <int> <dbl> <dbl> <dbl> <dbl> <dbl>    <dbl>
1 spbin2    218     3     3  674.  680.  680.  690. -337.    198.
2 spbin     218     3     3  676.  682.  683.  693. -338.    176.
# i 1 more variable: pseudo.r.squared <dbl>

R> loocv(spbin)

# A tibble: 1 x 3
  bias  MSPE RMSPE
  <dbl> <dbl> <dbl>
1 0.0000206 0.156 0.394

R> loocv(spbin2)

# A tibble: 1 x 3
  bias  MSPE RMSPE
  <dbl> <dbl> <dbl>
1 -0.000261 0.146 0.382
```

- 333 The SPGLM with the "exponential" spatial covariance (`spbin`) has a slightly lower (better)
 334 deviance but slightly higher (worse) AIC, AICc, and BIC than the SPGLM with the
 335 "gaussian" spatial covariance (`spbin2`). Both SPGLMs have similar leave-one-out cross
 336 validation metrics, though the SPGLM with the "gaussian" spatial covariance has slightly
 337 lower (better) RMSPE. For practical purposes, these models fit similarly.
- 338 Frequently in spatial statistics, the difference in model fit between the best spatial model
 339 and worst spatial model is much smaller than the difference in model fit between the worst
 340 spatial model and the nonspatial model, implying that accounting for some form of spatial
 341 covariance is very beneficial. Two spatial covariance functions to consider starting with are the
 342 exponential and Gaussian, which have quite different origin behaviors (Figure 2), something
 343 Stein (1999) argues is important to characterize accurately.

344 3.3. Model Diagnostics

- 345 `spmodel` provides a suite of tools for model diagnostics. One is `augment()`, which augments
 346 the data used in the model with several model diagnostics (introduced in Section 2.3):

```
R> augment(spbin)

Simple feature collection with 218 features and 8 fields
Geometry type: POINT
Dimension:      XY
Bounding box:  xmin: 269085 ymin: 1416151 xmax: 419057.4 ymax: 1541016
Projected CRS: NAD83 / Alaska Albers
# A tibble: 218 x 9
```

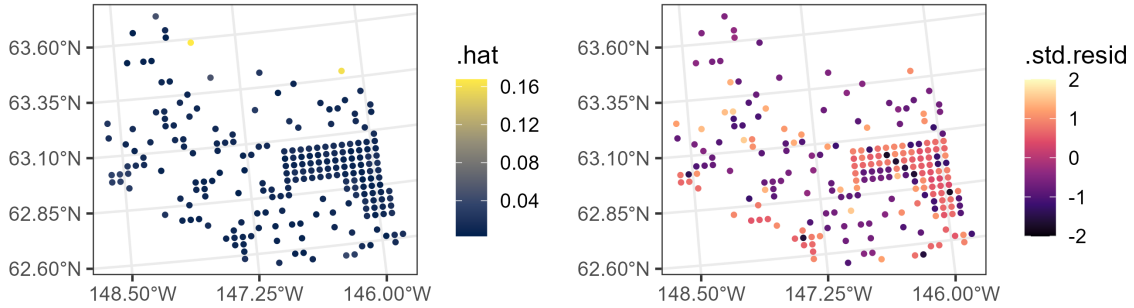


Figure 4: Moose presence model diagnostics, including leverage values (left) and standardized residuals (right).

```

presence elev strat .fitted .resid      .hat   .cooksdi .std.resid
* <fct>    <dbl> <chr> <dbl> <dbl> <dbl>    <dbl>
1 0        469. L     -1.95 -0.516 0.0476 0.00465 -0.528
2 0        362. L     -2.70 -0.361 0.0123 0.000548 -0.363
3 0        173. M     -1.96 -0.514 0.00455 0.000405 -0.516
4 0        280. L     -3.15 -0.290 0.00413 0.000117 -0.291
5 0        620. L     -1.19 -0.728 0.168 0.0427 -0.798
6 0        164. M     -1.71 -0.576 0.00534 0.000598 -0.578
7 0        164. M     -1.60 -0.606 0.00576 0.000714 -0.608
8 0        186. L     -2.50 -0.397 0.00439 0.000233 -0.398
9 0        362. L     -1.88 -0.532 0.0239 0.00237 -0.539
10 0       430. L    -1.54 -0.623 0.0497 0.00713 -0.639
# i 208 more rows
# i 1 more variable: geometry <POINT [m]>
```

347 The fitted values (`.fitted`) can be returned on either the link ($\hat{\mathbf{w}}$) or response ($f^{-1}(\hat{\mathbf{w}})$)
 348 scale and the residuals (`.resid`) can be deviance, Pearson, or response residuals. The default
 349 fitted values are on the link scale and the default residuals are deviance residuals. Also
 350 returned by `augment()` are the leverage (`.hat`), Cook's distance (`.cooksdi`), and standardized
 351 residuals (`.std.resid`) described in Section 2.3. A benefit of using `augment()` when `data` is
 352 an `sf` object is that the output is also an `sf` object, which makes it straightforward to create
 353 spatial diagnostic plots (Figure 4). Standard R helpers (e.g., `fitted()`, `residuals()`) are
 354 also available to extract model diagnostics from the model object.

355 The `plot()` function can also be used to return similar diagnostics as from `lm()` and `glm()`,
 356 with additional tools for diagnosing spatial covariance. For example, we can inspect Cook's
 357 distance values and the empirical spatial covariance as a function of distance with (Figure 5):

```
R> plot(spbin, which = c(4, 7))
```

358 The `varcomp()` function partitions model variability into several different components, helping
 359 to elucidate the model's structure:

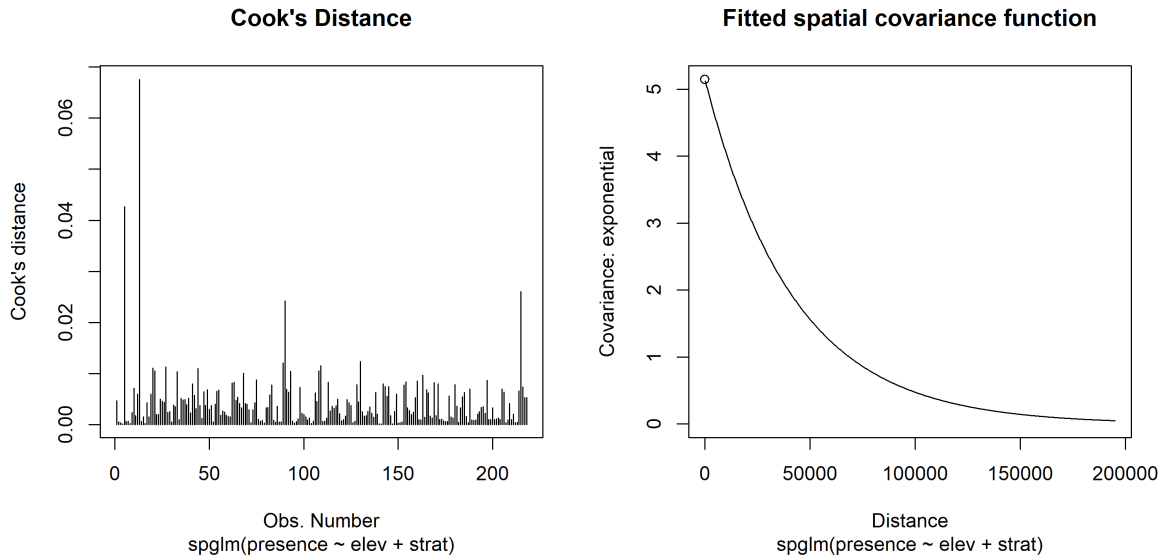


Figure 5: Moose presence model diagnostics, including Cook's distance (left) and the fitted spatial covariance as a function of distance (right).

```
R> varcomp(spbin)
```

```
# A tibble: 3 x 2
  varcomp      proportion
  <chr>          <dbl>
1 Covariates (PR-sq) 0.0627
2 de             0.937
3 ie             0.000236
```

360 The pseudo R-squared (PR^2) is reported in the first row. The remaining variability ($1 - PR^2$)
 361 is allocated proportionally to `de` and `ie` according to σ_{de}^2 and σ_{ie}^2 . This variability partitioning
 362 is a useful tool that helps quantify how much the explanatory variables, residual spatial
 363 variance, and residual nonspatial variance contribute to model fit; as with PR^2 , it should not
 364 be used for model comparison, but rather as a helpful model diagnostic.

365 3.4. Prediction

366 We can predict the probability of moose presence at the locations in `moose_preds` using
 367 `predict()`:

```
R> predict(spbin, newdata = moose_preds)[1:5]
```

1	2	3	4	5
0.06664165	-0.79069107	-1.60387940	-0.83159357	1.38183928

368 By default, predictions are returned on the link scale, but this can be changed to the response
 369 scale via `type`:

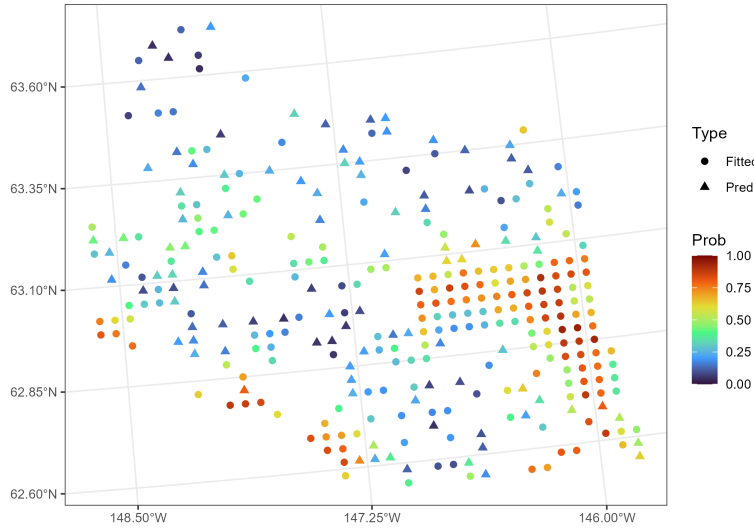


Figure 6: Moose presence probability fitted values and predictions. Fitted values are represented by circles and predictions by triangles.

```
R> predict(spbin, newdata = moose_preds, type = "response") [1:5]
```

	1	2	3	4	5
	0.5166542	0.3120203	0.1674401	0.3033082	0.7992862

370 Predictions on the response scale are visualized alongside the fitted values ($f^{-1}(\hat{\mathbf{w}})$) in
 371 Figure 6. Prediction intervals for the probability of moose presence (on the link scale) are
 372 returned by supplying `interval`:

```
R> predict(spbin, newdata = moose_preds, interval = "prediction") [1:5, ]
```

	fit	lwr	upr
1	0.06664165	-2.0374370	2.1707203
2	-0.79069107	-3.4758514	1.8944692
3	-1.60387940	-4.0953329	0.8875741
4	-0.83159357	-3.0704818	1.4072947
5	1.38183928	-0.7692107	3.5328893

373 We can alternatively use `augment()` to augment the prediction data with predictions. Argu-
 374 ments to `predict()` can also be passed to `augment()`:

```
R> augment(spbin, newdata = moose_preds, interval = "prediction")
```

```
Simple feature collection with 100 features and 5 fields
Geometry type: POINT
Dimension:      XY
Bounding box:  xmin: 269386.2 ymin: 1418453 xmax: 419976.2 ymax: 1541763
```

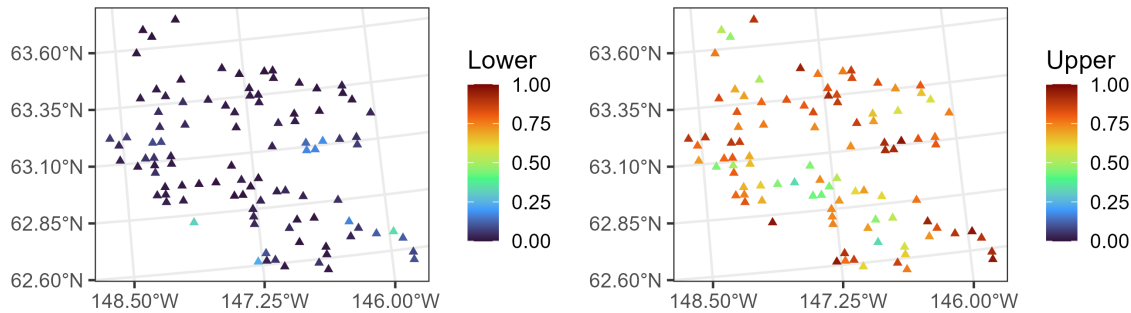


Figure 7: Moose presence 95% prediction interval lower bounds (left) and upper bounds (right).

```
Projected CRS: NAD83 / Alaska Albers
# A tibble: 100 x 6
  elev strat .fitted .lower   .upper      geometry
* <dbl> <chr>   <dbl>  <dbl>   <dbl>      <POINT [m]>
1 143. L     0.0666 -2.04    2.17 (401239.6 1436192)
2 324. L    -0.791  -3.48    1.89 (352640.6 1490695)
3 158. L    -1.60   -4.10    0.888 (360954.9 1491590)
4 221. M    -0.832  -3.07    1.41 (291839.8 1466091)
5 209. M     1.38   -0.769   3.53 (310991.9 1441630)
6 218. L    -2.59   -5.20    0.0177 (304473.8 1512103)
7 127. L    -2.73   -5.24   -0.220 (339011.1 1459318)
8 122. L    -2.32   -4.74    0.0920 (342827.3 1463452)
9 191. L    -1.17   -4.01    1.66 (284453.8 1502837)
10 105. L   -0.905  -3.05    1.24 (391343.9 1483791)
# i 90 more rows
```

³⁷⁵ By using `augment()` when `newdata` is an `sf` object, predictions and their corresponding
³⁷⁶ uncertainties are readily available for spatial mapping (Figure 7).

4. Additional applications

³⁷⁷ Throughout the remainder of this section, we briefly highlight some additional **spmodel** ca-
³⁷⁸ pabilities for SPGLMs. In Section 4.1, we fit Poisson and negative binomial models with
³⁷⁹ and without geometric anisotropy for the point-referenced moose count data. In Section 4.2,
³⁸⁰ we fit a Gamma model to the point-referenced lake conductivity data, showing how to fit a
³⁸¹ model with a partition factor, perform a spatial analysis of variance (ANOVA), and estimate
³⁸² contrasts for models with interactions. In Section 4.3, we fit a binomial model to the areal
³⁸³ harbor seal trend data with a nonspatial random effect. Finally in Section 4.4, we fit beta
³⁸⁴ models to Texas voter turnout data, which can be treated as point-referenced or areal, and
³⁸⁵ use maximum likelihood to compare two models with different explanatory variables. Table 1
³⁸⁶ outlines, for each application, the section number, data set, family (i.e., response distribution),

Section	Data	Family	Geometry	Additional Features
4.1	Moose Counts	Poisson NBinomial	Point	Geometric Anisotropy
4.2	Lake Conductivity	Gamma	Point	Partition Factor ANOVA Contrasts
4.3	Harbor Seals	Binomial	Areal	Nonspatial Random Effects
4.4	Texas Voter Turnout	Beta	Point Areal	Likelihood-Ratio Test

Table 1: Section number, data set, family, geometry type, and additional features for each application.

387 geometry type (point-referenced or areal), and additional **spmodel** features highlighted.

388 4.1. Modeling moose counts in Alaska, USA

389 In addition to moose presence, moose counts are also recorded in `moose` (Figure 8). The
 390 Poisson and negative binomial response distributions can be used to model SPGLMs for count
 391 data. The Poisson distribution mean is equal to its variance, while the negative binomial has
 392 an extra parameter to accommodate overdispersion (where the variance is larger than the
 393 mean). Using a spherical spatial covariance function, we may fit both a Poisson and negative
 394 binomial SPGLM changing the `family` argument:

```
R> sppois <- spglm(
+   formula = count ~ elev + strat,
+   family = poisson,
+   data = moose,
+   spcov_type = "spherical"
+ )
R> spnb <- update(sppois, family = nbomial)
```

395 Because the Poisson and negative binomial distributions have the same response support
 396 (nonnegative integers), we can compare them using AIC, AICc, or BIC:

```
R> BIC(sppois, spnb)
```

	df	BIC
sppois	3	1344.574
spnb	4	1343.105

397 Implicit in our spatial covariance functions thus far has been an assumption of geometric
 398 isotropy. A spatial covariance function is geometrically isotropic if it decays with distance
 399 at the same rate in all directions (Figure 9; left). A spatial covariance is geometrically
 400 anisotropic if it decays with distance at different rates in different directions (Figure 9; right).

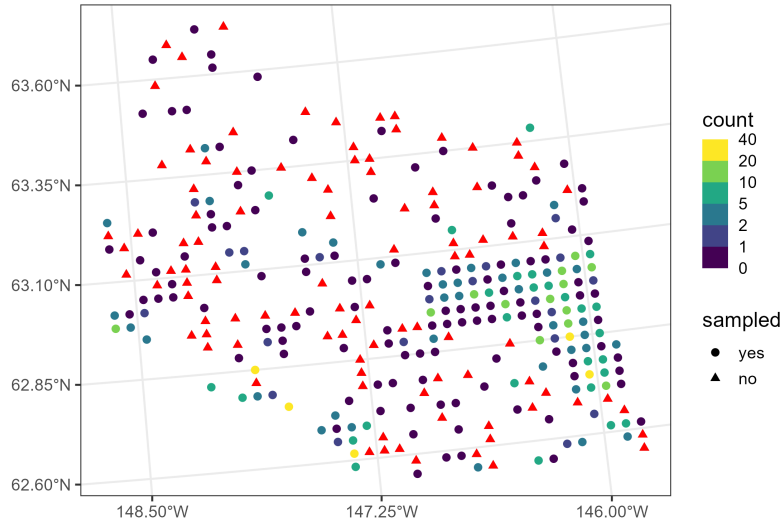


Figure 8: Moose counts in Alaska. Circles represent moose counts (based on color) and triangles represent locations at which mean count predictions are desired.

401 Geometric anisotropy is formally incorporated by rotating and scaling original coordinates,
402 yielding transformed coordinates that are geometrically isotropic:

$$\begin{bmatrix} x^* \\ y^* \end{bmatrix} = \begin{bmatrix} 1 & 0 \\ 0 & 1/\omega \end{bmatrix} \begin{bmatrix} \cos(\alpha) & \sin(\alpha) \\ -\sin(\alpha) & \cos(\alpha) \end{bmatrix} \begin{bmatrix} x \\ y \end{bmatrix}.$$

403 The parameters ω and α controls the scaling and rotation, respectively, of the major and
404 minor axes of a level curve of equal spatial covariance (Figure 9). Using these transformed
405 coordinates, the partial sill (σ_{de}^2), nugget (σ_{ie}^2), and range (ϕ) parameters are estimated. We
406 accommodate geometric anisotropy by supplying `anisotropy`:

```
R> sppois_anis <- update(sppois, anisotropy = TRUE)
R> spnb_anis <- update(spnb, anisotropy = TRUE)
```

407 According to BIC, the spatial negative binomial model with geometric anisotropy performs
408 best:

```
R> BIC(sppois, spnb, sppois_anis, spnb_anis)
```

	df	BIC
sppois	3	1344.574
spnb	4	1343.105
sppois_anis	5	1341.143
spnb_anis	6	1339.714

409 The `plot()` function can be used to visualize the anisotropy (Figure 9):

```
R> plot(spnb, which = 8)
R> plot(spnb_anis, which = 8)
```

410 The spatial covariance is strongest in a northwest-southeast direction and weakest in the
411 northeast-southwest direction (Figure 9), which is intuitive given the similar patterns in moose
412 counts from Figure 8.

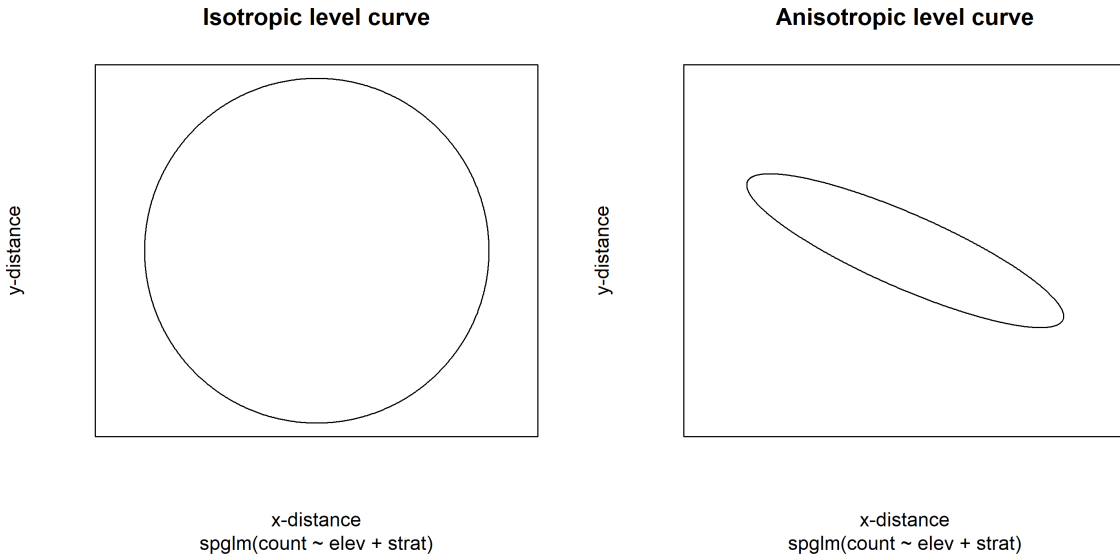


Figure 9: Level curves of equal spatial covariance for the negative binomial moose count models. The ellipse is centered at zero distance in the x-direction and y-direction, and points along the ellipse have equal levels of spatial covariance. In the isotropic level curve (left), spatial covariance decays equally in all directions. In the anisotropic level curve (right), spatial covariance decays fastest in the northeast-southwest direction and slowest in the northwest-southeast direction (this pattern can be seen in the observed counts).

413 4.2. Modeling lake conductivity in Southwest, USA

414 The `lake` data in `spmodel` contains climate and chemical data for several lakes in four south-
415 western states in the United States: Arizona, Colorado, Nevada, and Utah. We desire an
416 SPGLM that characterizes the effect of temperature, state, and lake origin (whether the lake
417 is naturally occurring or human made) on lake conductivity. Conductivity is a measure of
418 dissolved ions (measured here in water), which is important for various physical, chemical,
419 and biological processes. Chemical data are often heavily right-skewed, so we model them
420 using an SPGLM assuming a Gamma distribution for the response. The `log_cond` variable
421 in `lake` is the logarithm of conductivity, which we dynamically exponentiate within `formula`
422 so that it is on the original scale:

```
R> spgam <- spglm(
+   formula = exp(log_cond) ~ temp * state + origin,
+   family = "Gamma",
+   data = lake,
+   spcov_type = "cauchy",
+   partition_factor = ~ year
+ )
```

- 423 We model conductivity as a function of temperature, state, and lake origin, and we allow
 424 the effect of temperature to vary by state (`temp:state` interaction). The `year` partition
 425 factor (specified via `partition_factor`) restricts spatial covariance to be nonzero only for
 426 observations sampled during the same year. Data were collected in 2012 and 2017, so this
 427 partition factor assumes independence between observations in 2012 and 2017. While we used
 428 the partition factor here illustratively, more generally, the utility of partition factors can be
 429 highly context dependent.
- 430 When categorical variables have more than two levels, the default reference group contrasts
 431 are not well-suited to assess the variable's overall significance:

```
R> summary(spgam)
```

```
Call:
spglm(formula = exp(log_cond) ~ temp * state + origin, family = "Gamma",
      data = lake, spcov_type = "cauchy", partition_factor = ~year)

Deviance Residuals:
    Min      1Q   Median      3Q      Max
-1.35762 -0.20796 -0.03706  0.17869  1.10616

Coefficients (fixed):
            Estimate Std. Error z value Pr(>|z|)
(Intercept) 3.59325   0.50058  7.178 7.06e-13 ***
temp        0.15182   0.03006  5.051 4.39e-07 ***
stateCO     -0.03214   0.56098 -0.057  0.95432
stateNV      0.75664   0.66851  1.132  0.25771
stateUT     -0.19696   0.55916 -0.352  0.72466
originNATURAL 0.08313   0.21988  0.378  0.70538
temp:stateCO 0.13679   0.04808  2.845  0.00444 **
temp:stateNV 0.01882   0.05820  0.323  0.74645
temp:stateUT 0.20015   0.04846  4.131 3.62e-05 ***

---
Signif. codes:  0 '***' 0.001 '**' 0.01 '*' 0.05 '.' 0.1 ' ' 1

Pseudo R-squared: 0.7061

Coefficients (cauchy spatial covariance):
      de      ie      range      extra
2.069e-02 2.952e-01 4.119e+06 5.645e-01

Coefficients (Dispersion for Gamma family):
dispersion
      3.761
```

- 432 A more effective approach is to use an analysis of variance (ANOVA), which is well-suited to
 433 assess the overall significance of each variable:

```
R> anova(spgam)
```

Analysis of Variance Table

```
Response: exp(log_cond)
          Df  Chi2 Pr(>Chi2)
(Intercept) 1 51.5270 7.062e-13 ***
temp         1 25.5146 4.390e-07 ***
state        3  3.0747 0.3802528
origin       1  0.1429 0.7053819
temp:state   3 19.7668 0.0001897 ***
---
Signif. codes:  0 '***' 0.001 '**' 0.01 '*' 0.05 '.' 0.1 ' ' 1
```

- 434 The main effect for temperature and the temperature by state interaction are highly significant
 435 (*p* value < 0.001), while the main effects for state and lake origin are not significant.
 436 Variance inflation factors assess the degree to which standard errors $\hat{\beta}$ are inflated due to
 437 covariance among the columns of **X**. Generalized variance inflation factors can capture the
 438 variance inflation for subsets of **X** that may include categorical variables with more than two
 439 levels (Fox and Monette 1992):

```
R> library("car")
```

```
R> vif(spgam)
```

	GVIF	Df	GVIF ^{(1/(2*Df))}
temp	4.691914	1	2.166083
state	127.082397	3	2.242234
origin	1.264940	1	1.124695
temp:state	76.387383	3	2.059856

- 440 The GVIF^{1/2df} values for **temp**, **state**, and **temp:state** are just greater than two, which
 441 suggests moderate multicollinearity for these terms – unsurprising given the **temp:state**
 442 interaction in the model. The GVIF^{1/2df} for **origin** is close to one, which suggests little to
 443 no multicollinearity for this term.
 444 Because of the interaction between **temp** and **state**, contrasts that assess mean differences
 445 among states should condition upon a specific temperature value. By default, **emmeans** uses
 446 the mean temperature value (here, 7.63) to assess contrasts:

```
R> library("emmeans")
```

```
R> pairs(emmeans(spgam, ~ state | temp))
```

```
temp = 7.63:
contrast estimate    SE  df z.ratio p.value
AZ - CO     -1.012 0.337 Inf -3.004  0.0142
```

AZ - NV	-0.900	0.348	Inf	-2.584	0.0480
AZ - UT	-1.331	0.326	Inf	-4.082	0.0003
CO - NV	0.112	0.258	Inf	0.434	0.9727
CO - UT	-0.319	0.223	Inf	-1.427	0.4822
NV - UT	-0.431	0.244	Inf	-1.763	0.2915

Results are averaged over the levels of: origin

Degrees-of-freedom method: asymptotic

Results are given on the log (not the response) scale.

P value adjustment: tukey method for comparing a family of 4 estimates

- 447 Again, because of the interaction between `temp` and `state`, we should assess temperature
 448 trends separately for each state:

```
R> emtrends(spgam, ~ state, var = "temp")
```

state	temp.trend	SE	df	asymp.LCL	asymp.UCL
AZ	0.152	0.0301	Inf	0.0929	0.211
CO	0.289	0.0370	Inf	0.2161	0.361
NV	0.171	0.0504	Inf	0.0718	0.270
UT	0.352	0.0372	Inf	0.2791	0.425

Results are averaged over the levels of: origin

Degrees-of-freedom method: asymptotic

Results are given on the exp (not the response) scale.

Confidence level used: 0.95

449 4.3. Modeling harbor seal trends in Alaska, USA

- 450 The `seal` data in `spmodel` contains harbor seal abundance trends for two different harbor
 451 seal stocks (genetically distinct populations). While the `moose` and `lake` data were point-
 452 referenced, the `seal` data are areal. Each polygon in the `seal` data represents a distinct
 453 harbor seal haulout region (Figure 10). A haulout region is an area of coastal rocks that
 454 harbor seals go to rest, molt, and give birth.

- 455 For each polygon, a Poisson regression was used to quantify the mean trend in abundance
 456 over approximately 30 years (Ver Hoef, Peterson, Hooten, Hanks, and Fortin 2018). If the
 457 logarithm of mean abundance trends (`log_trend`) is negative (positive), it means abundance
 458 is decreasing (increasing). We use a binomial SPGLM to quantify the likelihood that mean
 459 abundance trends are decreasing:

```
R> is_decreasing <- seal$log_trend < 0
R> spbin <- spgautor(
+   formula = is_decreasing ~ 1,
+   family = binomial,
+   data = seal,
+   spcov_type = "car",
```

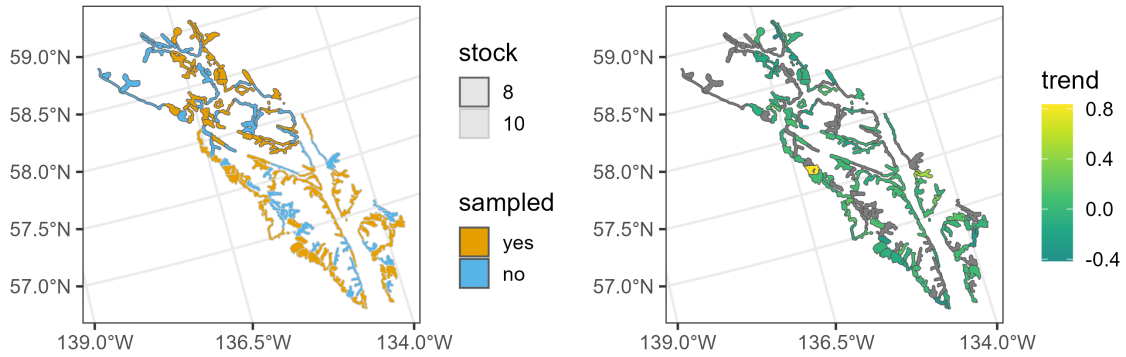


Figure 10: Seal trend distribution in Alaska. Observed and missing seal polygons by stock (left) and observed log seal trends (right).

```
+   random = ~ stock
+ )
```

To model spatial dependence, we used a conditional autoregressive function. Conditional and simultaneous autoregressive functions characterize spatial distance through neighborhood relationships (rather than Euclidean distance) and have `spcov_type` values of "car" and "sar", respectively. By default, Queen's distance is used to determine whether two sites are neighbors, though custom neighborhood matrices can be passed via `W`. Row standardization is also assumed by default; this can be changed via `row_st`. Using `random`, we also specified a nonspatial random effect for seal stock, which implies seals belonging to the same stock share extra covariance. The `random` argument uses similar syntax as `lme4` (Bates, Mächler, Bolker, and Walker 2015) and `nlme` (Pinheiro and Bates 2006) to specify nonspatial random effects.

Tidying the model reveals the estimates and confidence intervals on the log odds scale:

```
R> tidy(spbin, conf.int = TRUE)

# A tibble: 1 x 7
  term      estimate std.error statistic p.value conf.low conf.high
  <chr>      <dbl>     <dbl>     <dbl>    <dbl>    <dbl>    <dbl>
1 (Intercept)  0.340     0.673     0.506    0.613   -0.979    1.66
```

Back-transforming the confidence interval to the probability scale yields:

```
R> emmeans(spbin, ~ 1, type = "response")

 1       prob      SE  df asympt.LCL asympt.UCL
 overall 0.584 0.164 Inf      0.273      0.84

Degrees-of-freedom method: asymptotic
Confidence level used: 0.95
Intervals are back-transformed from the logit scale
```

⁴⁷¹ The **SE** column is the standard error on the response scale obtained from the delta method
⁴⁷² (Oehlert 1992; Ver Hoef 2012).

⁴⁷³ In contrast to point-referenced data, prediction locations for areal data must be specified
⁴⁷⁴ at the time of model fitting, as they affect the spatial covariance function's neighborhood
⁴⁷⁵ structure. Prediction locations whose response values have an **NA** (i.e., missing) value are
⁴⁷⁶ converted into a **newdata** object that is stored in the model output. For example, rows one
⁴⁷⁷ and nine are locations without seal trends, meaning they are not used in model fitting but
⁴⁷⁸ are desired for prediction:

```
R> seal
```

```
Simple feature collection with 149 features and 2 fields
Geometry type: POLYGON
Dimension:      XY
Bounding box:  xmin: 913618.8 ymin: 855730.2 xmax: 1221859 ymax: 1145054
Projected CRS: NAD83 / Alaska Albers
# A tibble: 149 x 3
  log_trend stock                         geometry
  * <dbl>   <fct>                        <POLYGON [m]>
1 NA        8    ((1035002 1054710, 1035002 1054542, 1035002 105354~
2 -0.282    8    ((1037002 1039492, 1037006 1039490, 1037017 103949~
3 -0.00121   8    ((1070158 1030216, 1070185 1030207, 1070187 103020~
4  0.0354    8    ((1054906 1034826, 1054931 1034821, 1054936 103482~
5 -0.0160    8    ((1025142 1056940, 1025184 1056889, 1025222 105683~
6  0.0872    8    ((1026035 1044623, 1026037 1044605, 1026072 104461~
7 -0.266    8    ((1100345 1060709, 1100287 1060706, 1100228 106070~
8  0.0743    8    ((1030247 1029637, 1030248 1029637, 1030265 102964~
9 NA        8    ((1043093 1020553, 1043097 1020550, 1043101 102055~
10 -0.00961   8    ((1116002 1024542, 1116002 1023542, 1116002 102254~
# i 139 more rows
```

⁴⁷⁹ Then, **predict()** can be called without having to specify **newdata**:

```
R> predict(spin, type = "response", interval = "prediction")[1:5, ]
```

	fit	lwr	upr
1	0.6807677	0.3863736	0.8783808
9	0.5945680	0.2467634	0.8678078
13	0.6189055	0.2974432	0.8616799
15	0.6040102	0.2921802	0.8493132
18	0.6375700	0.3356282	0.8596641

⁴⁸⁰ We could have alternatively used a (geostatistical) SPGLM via **spglm()**. When areal data are
⁴⁸¹ used with **spglm()**, the centroids of each polygon are used as the point-referenced coordinates.
⁴⁸² We further explore comparisons between point-referenced and areal data in the next example.

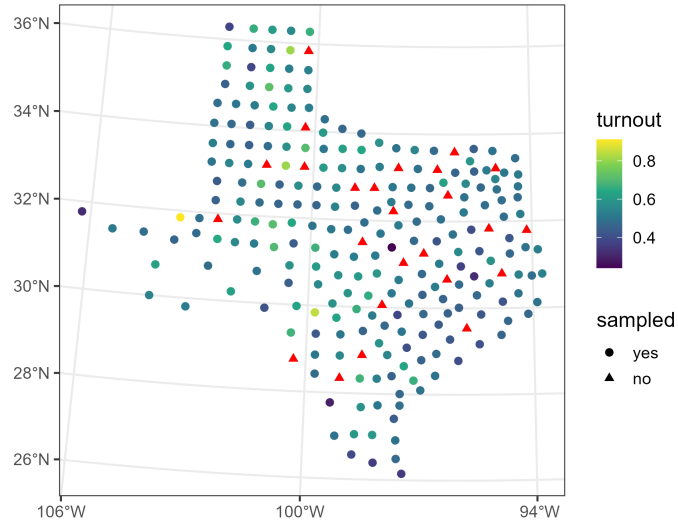


Figure 11: Proportion of voter turnout in Texas for the 1980 presidential election. Circles represent voter turnout (based on color) and triangles represent locations at which voter turnout predictions are desired.

483 4.4. Modeling voter turnout in Texas, USA

484 The `texas` data in `spmodel` contains voter turnout data for Texas counties in the 1980 United
 485 States Presidential Election (Bivand, Nowosad, and Lovelace 2024). The data are point-
 486 referenced, with polygon centroids representing the spatial location of each county (Figure 11).
 487 Beta regression is a GLM used to model rate and proportion data in the $(0, 1)$ interval (Ferrari
 488 and Cribari-Neto 2004; Cribari-Neto and Zeileis 2010). We model voter turnout rates as a
 489 function of mean log income of county residents using an SPGLM assuming a beta distributed
 490 response variable:

```
R> spbeta_geo <- spglm(
+   formula = turnout ~ log_income,
+   family = "beta",
+   data = texas,
+   spcov_type = "matern"
+ )
```

491 Alternatively, we could use an autoregressive model to fit the model, constructing a neighbor-
 492 hood matrix by assuming centroids within `cutoff` of one another are neighbors:

```
R> spbeta_auto <- spgautor(
+   formula = turnout ~ log_income,
+   family = "beta",
+   data = texas,
+   spcov_type = "car",
+   cutoff = 1e5
+ )
```

493 According to AIC, the SPGLM for point-referenced data is preferred:

```
R> AIC(spbeta_geo, spbeta_auto)
```

df	AIC
spbeta_geo	5 -44.53113
spbeta_auto	3 -22.46104

494 The default estimation method in **spmodel** for SPGLMs is restricted maximum likelihood
 495 (REML), while maximum likelihood (ML) can also be used. A benefit of benefit of REML
 496 is that it can yield unbiased estimates of covariance parameters (Cressie and Lahiri 1993),
 497 but a drawback is that likelihood-based statistics are only valid for model comparison when
 498 the models have the same explanatory variable and fixed effect structure (because the error
 499 contrasts used to construct the REML likelihood change based on \mathbf{X} and β). In contrast, ML
 500 estimators are generally biased for covariance parameters, though in practice this bias tends
 501 to be small. Moreover, when using ML, likelihood-based comparisons are valid for models
 502 having different explanatory variable and fixed effect structures. Using ML, we can evaluate
 503 the significance of log income on voter turnout using a likelihood ratio test:

```
R> spbeta_full_ml <- update(spbeta_geo, estmethod = "ml")
R> spbeta_red_ml <- update(spbeta_geo, estmethod = "ml", formula = turnout ~ 1)
R> anova(spbeta_full_ml, spbeta_red_ml)
```

Likelihood Ratio Test

```
Response: turnout
          Df   Chi2 Pr(>Chi2)
spbeta_red_ml vs spbeta_full_ml 1 23.155 1.494e-06 ***
---
Signif. codes: 0 '***' 0.001 '**' 0.01 '*' 0.05 '.' 0.1 ' ' 1
```

504 The likelihood ratio test provides strong evidence that log income is significantly related
 505 to voter turnout (p value < 0.001). Alternatively, we could have instead used a different
 506 likelihood-based statistic like AIC:

```
R> AIC(spbeta_full_ml, spbeta_red_ml)
```

df	AIC
spbeta_full_ml	7 -31.25900
spbeta_red_ml	6 -10.10354

507 The AIC also prefers the full model, suggesting that log income is important for predicting
 508 voter turnout.

5. Discussion

SPGLMs are fit in **spmodel** using a novel application of the Laplace approximation that simultaneously marginalizes over the latent (i.e., unobserved) random effects and the fixed effects. **spmodel**'s `spglm()` (for point-referenced data) and `spgautor()` (for areal data) fit SPGLMs that are similar in structure and syntax as base R's `glm()` function, easing the transition from GLMs to SPGLMs for practitioners. The `spglm()` and `spgautor()` functions support six response distributions for binary, count, and skewed data and 20 spatial covariance functions. **spmodel** has a suite of tools for data visualization, inference, model diagnostics, and prediction, providing a framework that can be used for all stages of a data analysis. There are many additional **spmodel** features that are not covered here, including fitting multiple models simultaneously, fixing spatial covariance and dispersion parameters at known values, fitting models to large non-Gaussian data having thousands of observations via spatial indexing (Ver Hoef, Dumelle, Higham, Peterson, and Isaak 2023), incorporating spatial dependence in machine learning (e.g., random forests; Breiman (2001)), simulating spatially dependent data (e.g., `spbinom()`, `sprpois()`, etc.), and more. Further details are provided by <https://CRAN.R-project.org/package=spmodel> and links therein.

Data and code availability

The results in this manuscript were obtained using R 4.4.0 with the **spmodel** 0.11.1 package. Figures were created using the `ggplot2` 3.5.1 package (Wickham 2016) and base R. All writing and code associated with this manuscript is available for viewing and download on GitHub at <https://github.com/USEPA/spmodel.glm.manuscript>. All data used are part of the **spmodel** R package available for download from CRAN at <https://CRAN.R-project.org/package=spmodel>. Results were obtained using R 4.4.0 with the **spmodel** 0.11.1 package. Figures were created using the `ggplot2` 3.5.1 package (Wickham 2016) and base R.

Acknowledgments

We would like to genuinely thank the associate editor, anonymous reviewers, and editorial staff for significant support and feedback that greatly improved the manuscript. The views expressed in this article are those of the author(s) and do not necessarily represent the views or policies of the U.S. government, U.S. Environmental Protection Agency or the National Oceanic and Atmospheric Administration. Mention of trade names or commercial products does not constitute endorsement or recommendation for use.

References

- Akaike H (1974). “A New Look at the Statistical Model Identification.” *IEEE Transactions on Automatic Control*, **19**(6), 716–723.
- Anderson SC, Ward EJ, English PA, Barnett LAK, Thorson JT (2024). “sdmTMB: An R package for Fast, Flexible, and User-Friendly Generalized Linear Mixed Effects Models with Spatial and Spatiotemporal Random Fields.” *bioRxiv*, **2022.03.24.485545**. doi: [10.1101/2022.03.24.485545](https://doi.org/10.1101/2022.03.24.485545).

- 543 Bachl FE, Lindgren F, Borchers DL, Illian JB (2019). “inlabru: An R Package for Bayesian
 544 Spatial Modelling from ecological survey data.” *Methods in Ecology and Evolution*, **10**,
 545 760–766. [doi:10.1111/2041-210X.13168](https://doi.org/10.1111/2041-210X.13168).
- 546 Bates D, Mächler M, Bolker B, Walker S (2015). “Fitting Linear Mixed-Effects Models Using
 547 lme4.” *Journal of Statistical Software*, **67**(1), 1–48. [doi:10.18637/jss.v067.i01](https://doi.org/10.18637/jss.v067.i01).
- 548 Bivand R, Nowosad J, Lovelace R (2024). *spData: Datasets for Spatial Analysis*. R package
 549 version 2.3.1, URL <https://CRAN.R-project.org/package=spData>.
- 550 Bolker BM, Brooks ME, Clark CJ, Geange SW, Poulsen JR, Stevens MHH, White JSS (2009).
 551 “Generalized Linear Mixed Models: A Practical Guide for Ecology and Evolution.” *Trends
 552 in Ecology & Evolution*, **24**(3), 127–135.
- 553 Bonat WH, Ribeiro Jr PJ (2016). “Practical Likelihood Analysis for Spatial Generalized
 554 Linear Mixed Models.” *Environmetrics*, **27**(2), 83–89.
- 555 Breiman L (2001). “Random Forests.” *Machine Learning*, **45**, 5–32.
- 556 Breslow NE, Clayton DG (1993). “Approximate Inference in Generalized Linear Mixed Mod-
 557 els.” *Journal of the American Statistical Association*, **88**(421), 9–25.
- 558 Brooks ME, Kristensen K, van Benthem KJ, Magnusson A, Berg CW, Nielsen A, Skaug
 559 HJ, Maechler M, Bolker BM (2017). “glmmTMB Balances Speed and Flexibility Among
 560 Packages for Zero-Inflated Generalized Linear Mixed Modeling.” *The R Journal*, **9**(2),
 561 378–400. [doi:10.32614/RJ-2017-066](https://doi.org/10.32614/RJ-2017-066).
- 562 Bürkner PC (2017). “brms: An R package for Bayesian Multilevel Models Using Stan.”
 563 *Journal of Statistical Software*, **80**, 1–28.
- 564 Chambers JM, Hastie TJ (eds.) (1992). *Statistical Models in S*. Chapman & Hall, London.
- 565 Cook RD (1979). “Influential Observations in Linear Regression.” *Journal of the American
 566 Statistical Association*, **74**(365), 169–174.
- 567 Cook RD, Weisberg S (1982). *Residuals and Influence in Regression*. New York: Chapman
 568 and Hall.
- 569 Cressie N (1990). “The Origins of Kriging.” *Mathematical Geology*, **22**(3), 239–252.
- 570 Cressie N (1993). *Statistics for Spatial Data*. John Wiley & Sons.
- 571 Cressie N, Lahiri SN (1993). “The Asymptotic Distribution of REML Estimators.” *Journal
 572 of multivariate analysis*, **45**(2), 217–233.
- 573 Cribari-Neto F, Zeileis A (2010). “Beta Regression in R.” *Journal of statistical software*,
 574 **34**(1), 1–24.
- 575 Doser JW, Finley AO, Kéry M, Zipkin EF (2022). “spOccupancy: An R Package for Single-
 576 Species, Multi-Species, and Integrated Spatial Occupancy Models.” *Methods in Ecology and
 577 Evolution*, **13**(8), 1670–1678.

- 578 Doser JW, Finley AO, Kéry M, Zipkin EF (2024). “spAbundance: An R package for Single-
579 Species and Multi-Species Spatially Explicit Abundance Models.” *Methods in Ecology and
580 Evolution*, **15**(6), 1024–1033.
- 581 Dumelle M, Higham M, Ver Hoef JM (2023). “spmodel: Spatial Statistical Modeling and
582 Prediction in R.” *PLOS ONE*, **18**(3), e0282524.
- 583 Evangelou E, Zhu Z, Smith RL (2011). “Estimation and Prediction for Spatial Generalized
584 Linear Mixed Models Using High Order Laplace Approximation.” *Journal of Statistical
585 Planning and Inference*, **141**(11), 3564–3577.
- 586 Faraway JJ (2016). *Extending the Linear Model with R: Generalized Linear, Mixed Effects
587 and Nonparametric Regression Models*. CRC press.
- 588 Ferrari S, Cribari-Neto F (2004). “Beta Regression for Modelling Rates and Proportions.”
589 *Journal of Applied Statistics*, **31**(7), 799–815.
- 590 Finley AO, Banerjee S, Carlin BP (2007). “spBayes: An R Package for Univariate and
591 Multivariate Hierarchical Point-Referenced Spatial Models.” *Journal of Statistical Software*,
592 **19**(4), 1–24. URL <https://www.jstatsoft.org/article/view/v019i04>.
- 593 Finley AO, Datta A, Banerjee S (2022). “spNNGP R Package for Nearest Neighbor Gaussian
594 Process Models.” *Journal of Statistical Software*, **103**(5), 1–40. doi:[10.18637/jss.v103.i05](https://doi.org/10.18637/jss.v103.i05).
- 595 596 Fox J, Monette G (1992). “Generalized Collinearity Diagnostics.” *Journal of the American
597 Statistical Association*, **87**(417), 178–183.
- 598 Fox J, Weisberg S (2019). *An R Companion to Applied Regression*. Third edition. Sage,
599 Thousand Oaks CA. URL <https://www.john-fox.ca/Companion/>.
- 600 Harville DA (1974). “Bayesian inference for variance components using only error contrasts.”
601 *Biometrika*, **61**(2), 383–385.
- 602 Hoeting JA, Davis RA, Merton AA, Thompson SE (2006). “Model Selection for Geostatistical
603 Models.” *Ecological Applications*, **16**(1), 87–98.
- 604 Hughes J, Cui X (2020). *ngspatial: Fitting the Centered Autologistic and Sparse Spatial
605 Generalized Linear Mixed Models for Areal Data*. Frederick, MD. R package version 1.2-2.
- 606 James G, Witten D, Hastie T, Tibshirani R (2013). *An Introduction to Statistical Learning*.
607 Springer-Verlag.
- 608 Kuhn M, Silge J (2022). *Tidy Modeling with R*. O'Reilly Media, Inc.
- 609 Lee D (2013). “CARBayes: An R Package for Bayesian Spatial Modeling with Conditional
610 Autoregressive Priors.” *Journal of Statistical Software*, **55**(13), 1–24.
- 611 Lee Y, Nelder JA (1996). “Hierarchical Generalized Linear Models.” *Journal of the Royal
612 Statistical Society: Series B (Methodological)*, **58**(4), 619–656.
- 613 Lenth RV (2024). *emmeans: Estimated Marginal Means, aka Least-Squares Means*. R package
614 version 1.10.3, URL <https://CRAN.R-project.org/package=emmeans>.

- 615 Lindgren F, Rue H (2015). “Bayesian Spatial Modelling with R-INLA.” *Journal of Statistical
616 Software*, **63**, 1–25.
- 617 McCullagh P, Nelder JA (1989). *Generalized Linear Models, Second Edition*. Chapman and
618 Hall Ltd.
- 619 Montgomery DC, Peck EA, Vining GG (2021). *Introduction to Linear Regression Analysis*.
620 John Wiley & Sons.
- 621 Myers RH, Montgomery DC, Vining GG, Robinson TJ (2012). *Generalized Linear Models:
622 With Applications in Engineering and the Sciences*. John Wiley & Sons.
- 623 Nelder JA, Wedderburn RW (1972). “Generalized Linear Models.” *Journal of the Royal
624 Statistical Society A*, **135**(3), 370–384.
- 625 Oehlert GW (1992). “A Note on the Delta Method.” *The American Statistician*, **46**(1), 27–29.
- 626 Patterson D, Thompson R (1971). “Recovery of Inter-Block Information when Block Sizes
627 are Unequal.” *Biometrika*, **58**(3), 545–554.
- 628 Pebesma E (2018). “Simple Features for R: Standardized Support for Spatial Vector Data.”
629 *The R Journal*, **10**(1), 439–446. doi:10.32614/RJ-2018-009. URL <https://doi.org/10.32614/RJ-2018-009>.
- 631 Pinheiro J, Bates D (2006). *Mixed-Effects Models in S and S-PLUS*. Springer-Verlag Science
632 & Business Media.
- 633 R Core Team (2024). *R: A Language and Environment for Statistical Computing*. R Foun-
634 dation for Statistical Computing, Vienna, Austria. URL <https://www.R-project.org/>.
- 635 Rencher AC, Schaalje GB (2008). *Linear Models in Statistics*. John Wiley & Sons.
- 636 Robinson D, Hayes A, Couch S (2021). *broom: Convert Statistical Objects into Tidy Tibbles*.
637 R package version 0.7.6, URL <https://CRAN.R-project.org/package=broom>.
- 638 Ronnegard L, Shen X, Alam M (2010). “hglm: A Package for Fitting Hierarchical Generalized
639 Linear Models.” *The R Journal*, **2**(2), 20–28.
- 640 Rousset F, Ferdy JB (2014). “Testing Environmental and Genetic Effects in the Presence
641 of Spatial Autocorrelation.” *Ecography*, **37**(8), 781–790. URL <https://dx.doi.org/10.1111/ecog.00566>.
- 643 Sainsbury-Dale M, Zammit-Mangion A, Cressie N (2024). “Modeling Big, Heterogeneous,
644 Non-Gaussian Spatial and Spatio-Temporal Data Using FRK.” *Journal of Statistical Soft-
645 ware*, **108**, 1–39.
- 646 Schwarz G (1978). “Estimating the Dimension of a Model.” *The Annals of Statistics*, pp.
647 461–464.
- 648 Smith TJ, McKenna CM (2013). “A Comparison of Logistic Regression Pseudo R2 Indices.”
649 *General Linear Model Journal*, **39**(2), 17–26.

- 650 Stein ML (1999). *Interpolation of Spatial Data: Some Theory for Kriging*. Springer-Verlag
651 Science & Business Media.
- 652 Thorson JT, Anderson SC, Goddard P, Rooper CN (2025). “tinyVAST: R Package with an
653 Expressive Interface to Specify Lagged and Simultaneous Effects in Multivariate Spatio-
654 Temporal Models.” *Global Ecology and Biogeography*, **34**(4), e70035. doi:10.1111/geb.
655 70035. URL <https://doi.org/10.1111/geb.70035>.
- 656 Tobler WR (1970). “A Computer Movie Simulating Urban Growth in the Detroit Region.”
657 *Economic Geography*, **46**(sup1), 234–240.
- 658 Tredennick AT, Hooker G, Ellner SP, Adler PB (2021). “A Practical Guide to Selecting
659 Models for Exploration, Inference, and Prediction in Ecology.” *Ecology*, **102**(6), e03336.
- 660 Ver Hoef JM (2012). “Who Invented the Delta Method?” *The American Statistician*, **66**(2),
661 124–127.
- 662 Ver Hoef JM, Blagg E, Dumelle M, Dixon PM, Zimmerman DL, Conn PB (2024). “Marginal
663 Inference for Hierarchical Generalized Linear Mixed Models with Patterned Covariance
664 Matrices Using the Laplace Approximation.” *Environmetrics*, **35**(7), e2872. doi:10.1002/
665 env.2872.
- 666 Ver Hoef JM, Dumelle M, Higham M, Peterson EE, Isaak DJ (2023). “Indexing and Parti-
667 tioning the Spatial Linear Model for Large Data Sets.” *PLOS ONE*, **18**(11), e0291906.
- 668 Ver Hoef JM, Peterson EE, Hooten MB, Hanks EM, Fortin MJ (2018). “Spatial Autoregressive
669 Models for Statistical Inference From Ecological Data.” *Ecological Monographs*, **88**(1), 36–
670 59.
- 671 Wedderburn RW (1974). “Quasi-Likelihood Functions, Generalized Linear Models, and the
672 Gauss—Newton Method.” *Biometrika*, **61**(3), 439–447.
- 673 Wickham H (2016). *ggplot2: Elegant Graphics for Data Analysis*. Springer-Verlag, New York.
674 ISBN 978-3-319-24277-4. URL <https://ggplot2.tidyverse.org>.
- 675 Wolfinger R, O’Connell M (1993). “Generalized Linear Mixed Models: A Pseudo-Likelihood
676 Approach.” *Journal of Statistical Computation and Simulation*, **48**(3-4), 233–243.
- 677 Wolfinger R, Tobias R, Sall J (1994). “Computing Gaussian Likelihoods and their Derivatives
678 for General Linear Mixed Models.” *SIAM Journal on Scientific Computing*, **15**(6), 1294–
679 1310.
- 680 Wood SN (2017). *Generalized Additive Models: An Introduction with R*. CRC press.
- 681 Zimmerman DL, Ver Hoef JM (2024). *Spatial Linear Models for Environmental Data*. CRC
682 Press.

683 **Affiliation:**

684 Michael Dumelle
685 United States
686 Environmental Protection Agency
687 200 SW 35th St
688 Corvallis, OR, 97330
689 E-mail: Dumelle.Michael@epa.gov

690